Doctoral Dissertations

Student Theses and Dissertations

1970

# Some effects of OH groups on sodium silicate glasses

Mokhtar Sayed Maklad

SOME EFFECTS OF OH GROUPS ON SODIUM SILICATE GLASSES

by

MOKHTAR SAYED MAKLAD, 1941-

A DISSERTATION

Presented to the Faculty of the Graduate School of the

UNIVERSITY OF MISSOURI - ROLLA

In Partial Fulfillment of the Requirement for the Degree

DOCTOR OF PHILOSOPHY

in

CERAMIC ENGINEERING

T2413
82 pages
c.1

1970

<u>Advisor</u>

193979

## PUBLICATION THESIS OPTION

This thesis has been prepared in the style specified by the IX International Congress on Glass, Versailles, September 27-October 2, 1971.  Pages 1-37  will be published in the Proceedings of that Congress.  Appendix A was published in the Journal of the American Ceramic Society, Vol. 52, No. 9, pp 508-509, 1969.  Appendices B, C, D and E have been added for the purposes normal to thesis writing.

ABSTRACT

Glasses of various compositions in the $Na_2O-SiO_2$ system were prepared with different levels of OH concentration. Phase separation kinetics, thermal expansion, radiation induced optical absorption, and internal friction of these glasses were studied. The increase in OH content in these glasses was found to (a) enhance the rate of phase separation; (b) increase thermal expansion above the glass temperature and change the dilatometric softening temperature in a way that depends on microstructure; (c) increase the radiation induced optical absorption bands associated with positive hole centers and decrease those associated with electron trap centers; and, (d) decrease the low temperature alkali peak and increase the high temperature peak of internal friction. Structural changes responsible for the effect of very small amounts of OH on these properties are described. It is imperative to determine and consider OH content in the evaluation of properties which are so significantly affected by it.

## ACKNOWLEDGEMENTS

TABLE OF CONTENTS

TABLE OF CONTENTS (continued)

LIST OF FIGURES

LIST OF FIGURES (continued)

LIST OF FIGURES (continued)

LIST OF TABLES

## 1. INTRODUCTION

A small amount of dissolved OH groups can significantly influence many physical and technological properties of glasses. Increasing OH content generally increases electrical conductivity, density, refractive index, rate of crystallization, rate of diffusion, and thermal expansion, and decreases chemical durability and viscosity[1,2,44]. The lowering in viscosity is more pronounced in the transformation range than that at the softening point[3].

Several authors[1,2] have found that the solubility of water in glass is proportional to the square root of the partial pressure of water vapor; the dissolved water is present in the glass as OH groups and not as $H_2O$ molecules. The dissolution can be represented by $\equiv Si-O-Si \equiv + H_2O \rightarrow 2 \equiv Si-OH$.

Under extremely high pressure, water molecules can be incorporated in the structure. The OH concentration in glass can be determined quantitatively, using the characteristic infrared absorption bands or nuclear magnetic resonance (NMR).

Because water is present in glass in small amounts, its effect has been overlooked by many investigators when reporting quantitative relations of composition and properties. The purpose of this investigation is to obtain systematic

information on the effect of OH on some of the physical properties of well characterized, simple glasses; sodium silicate was selected for this study. Conversely, by studying the effect of OH groups in glass, one can get an insight into the structural environment and bonding around OH.

2.    EXPERIMENTAL PROCEDURE

2.1   GLASS PREPARATION

The glasses were prepared from reagent grade chemicals. $SiO_2$, provided by Bausch and Lomb, Inc., was a processed Quintus Quartz sand. After thorough mixing, and charging in a 250 ml platinum lined alumina crucible, the glass was melted in an electric furnace in the atmospheres described below. After holding overnight above the liquidus temperature, several melts of equal composition were treated differently to produce different levels of OH content. For the large "water" content glass, steam was bubbled in the melt using a mullite delivery tube, fitted with a platinum tube and sleeve, for 7 hours. To obtain the lowest "water" content, quenched and crushed glass was charged into a 30 ml platinum cricible and kept under vacuum ($\sim 20\mu$) in an alumina tube furnace heated to $200^{\circ}C$, held at $200^{\circ}C$ for 24 hours, at $600^{\circ}C$ for another 24 hours, above the liquidus temperature for one hour, and then quenched by lowering the crucible into a water cooled extension. Chemical analysis of the glasses indicated the loss of sodium did not exceed

0.2 mol % $Na_2O$. An intermediate OH level was achieved by melting under normal atmosphere where the melt was stirred with a platinum stirrer, to assure homogeneity, for 7 hours.

For phase separation studies, melts were cast between steel plates. Bars 5 x 1 x 1 cm were cast and annealed for thermal expansion and infrared measurements. Fibers about 0.5 mm in diameter were used for the internal friction measurements.

## 2.2 INFRARED MEASUREMENTS

To reduce the contribution of the water absorbed on the surfaces of the glass, the ground and polished samples were heated overnight under vacuum at $200°C$. Samples were then transferred to a desiccator, to be measured on a Perkin Elmer 377 I.R. spectrophotometer.

The absorption band position was determined from the spectra corresponding to the highest "water" content. The calculation was carried out in a similar way as reported by Goetz and Vosahlova[4], who had concluded that Beers-Lambert law was valid for determining "water" content up to 0.11 mol % in glass. We arbitrarily assumed similar absorption coefficients for sodium silicate glasses, 40 1/mole·cm for the $2.8\mu$ band and 55 1/mole·cm for the $3.6\mu$ bands, to make a semiquantitative comparison between glasses of the same composition.

## 2.3 TRANSMISSION ELECTRON MICROSCOPY

The glass to be examined was filed with a square 100 grit diamond file. To enhance contrast, the resulting flake was etched for 20 sec. in 5% hydrofluoric acid and for 10 sec. in 20% hydrochloric acid, agitated during the acid treatment, rinsed in distilled water, dried with a blast of clean compressed Freon* and scanned for areas thin enough to transmit electrons for observation.

A Hitachi HU-11A electron microscope was utilized for this study. Scanning was usually performed at 100 KV and 17,000 X magnification.

## 2.4 THERMAL EXPANSION MEASUREMENTS

The thermal expansion was measured with a horizontal Orton Automatic Recording dilatometer. From room temperature to the dilatometric softening point, expansion determinations were made at a heating rate about $0.5^{\circ}C/minute$ on samples two inches in length. The dilatometric softening point, was determined as the temperature at which viscous flow exactly counters thermal expansion during measurements; and the glass transition temperature (Tg) from the intersection of the line passing through the low temperature part of the curve with the line passing through the linear part above the Tg.

*EFFA duster - Ernest Fullam, Inc.

## 2.5 SPECTROPHOTOMETRIC AND IRRADIATION STUDIES

A Beckman DK-2A double beam ratio spectrophotometer was used for optical absorption measurement in the visible, uv and near infrared parts of the spectrum, before and after irradiation.

The x-radiation source for this study was a G.E. type EA-75 tungsten target x-ray tube operated at 50 KV and 40 milliampere. The absorbed dose rate was calculated from the "Los Alamos absorption coefficient tables for elements," the experimentally determined energy distribution of tungsten unfiltered radiation, and the density and thickness of the glass exposed, using a computer program as described elsewhere[5]. All specimens were irradiated at an absorbed dose rate of $2.2 \times 10^7$ rads per hour.

Bleaching was performed after irradiation using a short ultra-violet lamp ($\sim$220 m$\mu$).

## 2.6 INTERNAL FRICTION MEASUREMENTS

The internal friction measurements, as described elsewhere[5], were made on an annealed fiber approximately 60 to 70 mm long as an elastic member of an inverted torsion pendulum operating at 0.4 Hz. The pendulum was enclosed in a vacuum chamber, and pressure less than $10^{-2}\mu$ was maintained during the measurements.

## 3. RESULTS AND DISCUSSION

### 3.1 PHASE SEPARATION STUDIES

In the system $Na_2O-SiO_2$ subliquidus liquid-liquid immiscibility has been observed below about 20% $Na_2O$. In Fig. (1) both metastable and unstable regions are constructed from the reported data[7,8]. In the metastable region, phase separation occurs by nucleation and growth and is characterized by discrete particles dispersed within a continuous matrix. In the unstable region, phase separation should develop by spinodal decomposition, characterized by an interconnected microstructure. But phase connectivity could also arise from the intersecting growth of spheres starting from randomly oriented nuclei[9]. Also, in the opinion of Neilson[10], small angle x-ray scattering for sodium silicate glasses does not provide sufficient evidence to believe that spinodal decomposition always occurs or dominates in the unstable region. Haller and Macedo[11] proposed that during the growth stage the distorted spheres are rounded and forced to merge under the general driving force of reducing surface free energy and, more specifically, equalizing of interfacial curvature (Kelvin equation). Rounding by bulk diffusion or viscous flow are likely mechanisms to bring the surface of spheroids close together.

One composition in the metastable region was selected to study the effect of "OH" content on the separation
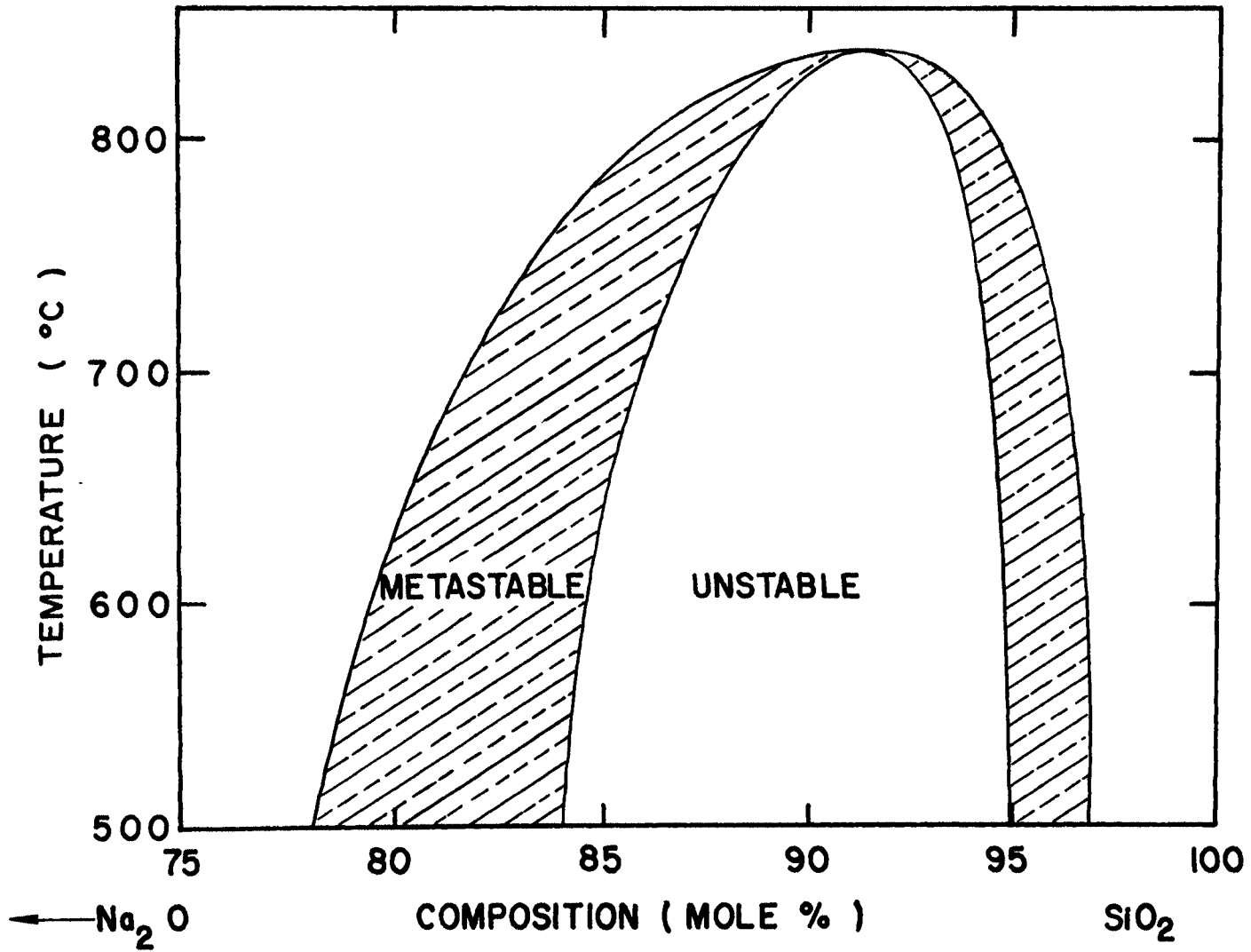
Figure 1. Subliquidus miscibility gap in the $Na_2O$. $SiO_2$ system.

kinetics. Fig. (2) shows transmission electron micrographs for the 15.5 mol % soda glass, illustrating the development of phase separation with time and with water content, at a temperature of 700°C. The micrographs for the quenched glasses (Fig. 2 A,D, and G), showed detectable phase separation with appearance of small particles with an average diameter of about 50 Å in high concentration. Some of these particles are in the stage of coalescence indicating that the growth stage had already started. In these quenched glasses a change in particle size with OH content is not noticeable. Upon heating, all glasses rapidly develop a high concentration of particles, the average size of the particle increases and the particle concentration decreases with time. The micrographs in Fig. 2B, E, and H show the effect of OH content after 20 minutes treatment at 700°C.

Generally, the average particle radius increases with increasing OH content, but the difference between the average size for the glass melted under normal atmosphere (2-E) and that for the vacuum melted glass (2-H), which has the lowest OH content, is very small. More particles are in the coalescence stage in the normal glass as compared to that in the glass melted under vacuum, after 20 and 180 minutes of heat treatment. The glass with the highest OH content (steam bubbling) showed a much larger increase in the size of the average particle and eventually was completely crystallized after 15.5 hours at 700°C,
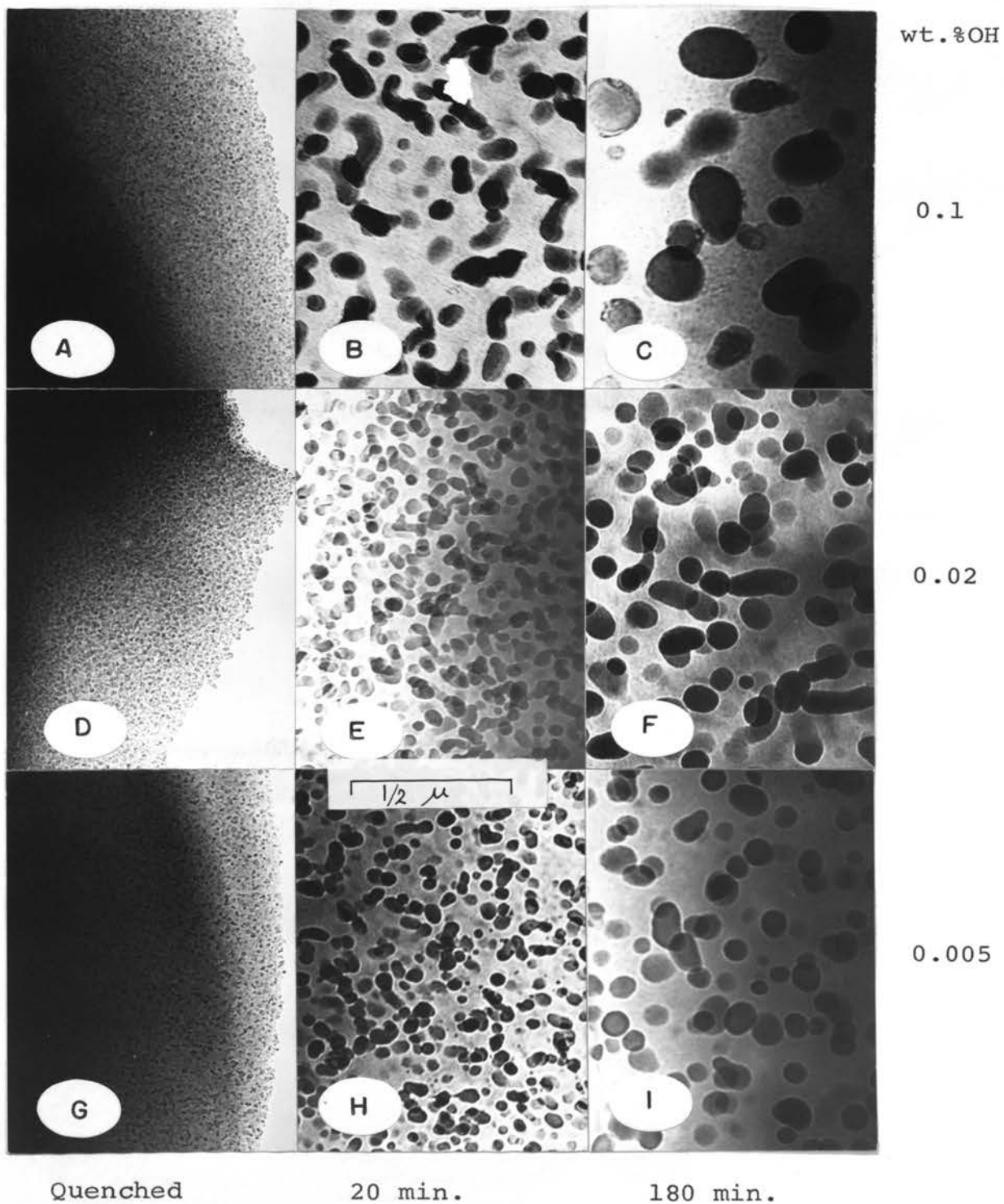
wt.%OH

Figure 2.  Transmission electron micrographs for various
heat treatments at 700°C of glasses with dif-
ferent OH contents, 15.5 mol % Na₂O

(A,B,C) 0.1 wt.%OH (steam)
(D,E,F) 0.02 wt.% OH (normal)
(G,H,I) 0.005 wt.%OH (vacuum)

while the other glasses were still noncrystalline. The
particle growth, in this case, more likely occurs by
impingement and rounding off the particle-matrix interface.
It is also noticeable that the concentration of the parti-
cles in the coalescence stage decreases with time, and as
the particle to particle distance increases, more parti-
cles become spherical.

This increase in particle size with OH content could be
explained by the increase in bulk diffusion and viscous
flow, at $700^{\circ}C$, which may enhance the growth by diffusion
or by impingement. We will see later that increasing the
water content decreases the glass temperature (Tg)(Fig.6)
and the temperature at which the glass network is mechani-
cally relaxed (Fig. 12). These observations suggest an
increase in diffusivity and viscous flow with increasing
OH content.

Fig. (3) shows the effect of time on the radius of the
average particle, at $700^{\circ}C$, for the three OH concentration
levels in the 15.5 mol % $Na_2O$ glass. The average particle
radius increases linearly with the cube root of time,
suggesting that the process is diffusion controlled. Simi-
lar observations are reported in the literature[9,12,13].
Generally, the slope of the straight lines increases with
increasing OH content (Fig. 3). The difference between the
glass with high OH content and other glasses is substantial.
But, the glass melted under normal atmosphere shows only a
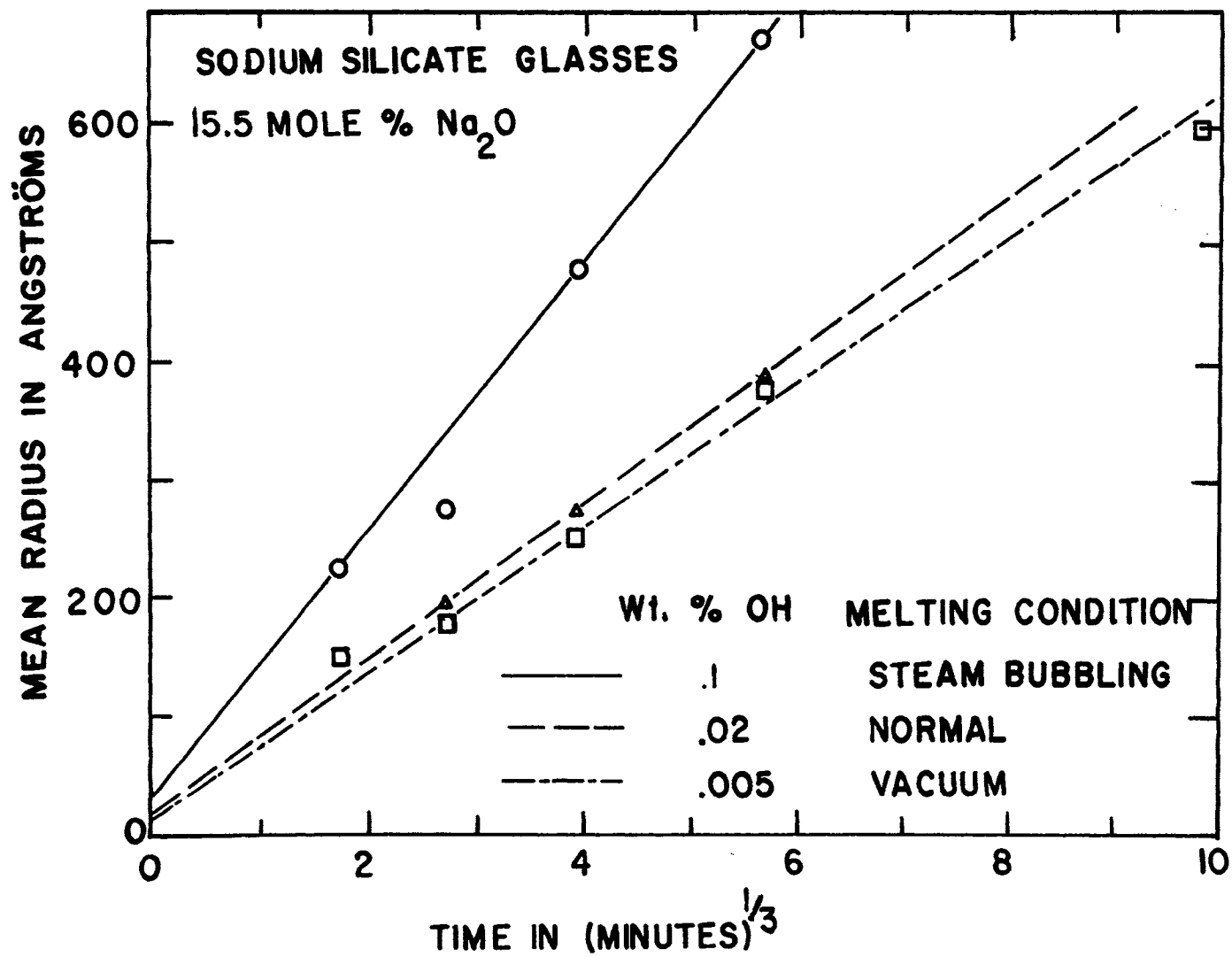
Figure 3. Variation with time of mean particle radius at 700°C, 15.5 mol % Na₂0 glasses, three levels of OH concentration.

slightly higher rate of increase of particle size, in comparison with that for the glass melted under vacuum.
It seems that some other factors must be counteracting
the effect of the "water" content. For instance, bulk
diffusion in the glass melted under vacuum might have been
increased by missing non-bridging oxygen. This would lead
to the high rate of particle size increase, unexpected
for such a low "water" content glass. Other evidence for
this suggestion will be discussed later in connection with
radiation effects and internal friction measurements.

We noticed that the water content of one glass melted
under normal atmosphere in the high humidity season was
about double that for the same glass prepared in the low
humidity season. Since phase separation was shown to be
sensitive to small changes in OH content of the glass, it
appears necessary that, in phase separation studies, the
water content of the glass be determined and considered,
as an important parameter influencing the kinetics of the
process.

In general, then, the introduction of a very small
concentration of OH groups enhances phase separation. It
seemed interesting to explore also the possibility of
suppressing phase separation by the introduction of suitable constituents in small concentrations. Glasses containing 13 mol % $Na_2O$, and 2 mol % of either ZnO or $ZrO_2$,
were heat treated at $700^{\circ}C$ for one hour. Fig. (4) shows

the transmission electron micrographs for these glasses after heat treatment. The base glass (Fig. 4-A) shows phase separation with a considerable degree of connectivity, characteristic for this composition, while the glass with ZnO (4-B) shows no connectivity but a few particles in the stage of coalescence. The larger particle size in the ZnO glass, as compared to the base glass, is due to the rounding off of the coalesced particles. This observation may suggest a larger interfacial energy in the ZnO glass. When $SiO_2$ is replaced by $ZrO_2$, the particles show little growth, and the microstructures of the quenched and heat treated glass are similar. This glass differed from the other glasses by not exhibiting opalescence after long time heat treatment. The substitution of these oxides not only decreases the rate of phase separation, but also affects the thermodynamic stability of the phase. This is reflected in the reduction in the size of the phase separation dome as we go into the ternary field.

## 3.2 THERMAL EXPANSION PROPERTIES

### 3.21 Thermal Expansion Characteristics and Glass Transition Temperature (Tg)

Fig. 5 illustrates the thermal expansion curves for two compositions in the system $Na_2O-SiO_2$. The 20.5 mol % $Na_2O$ glass shows the thermal expansion behavior for the metastable phase separation region, where silica-rich droplets occur in a soda-rich matrix. In this glass only
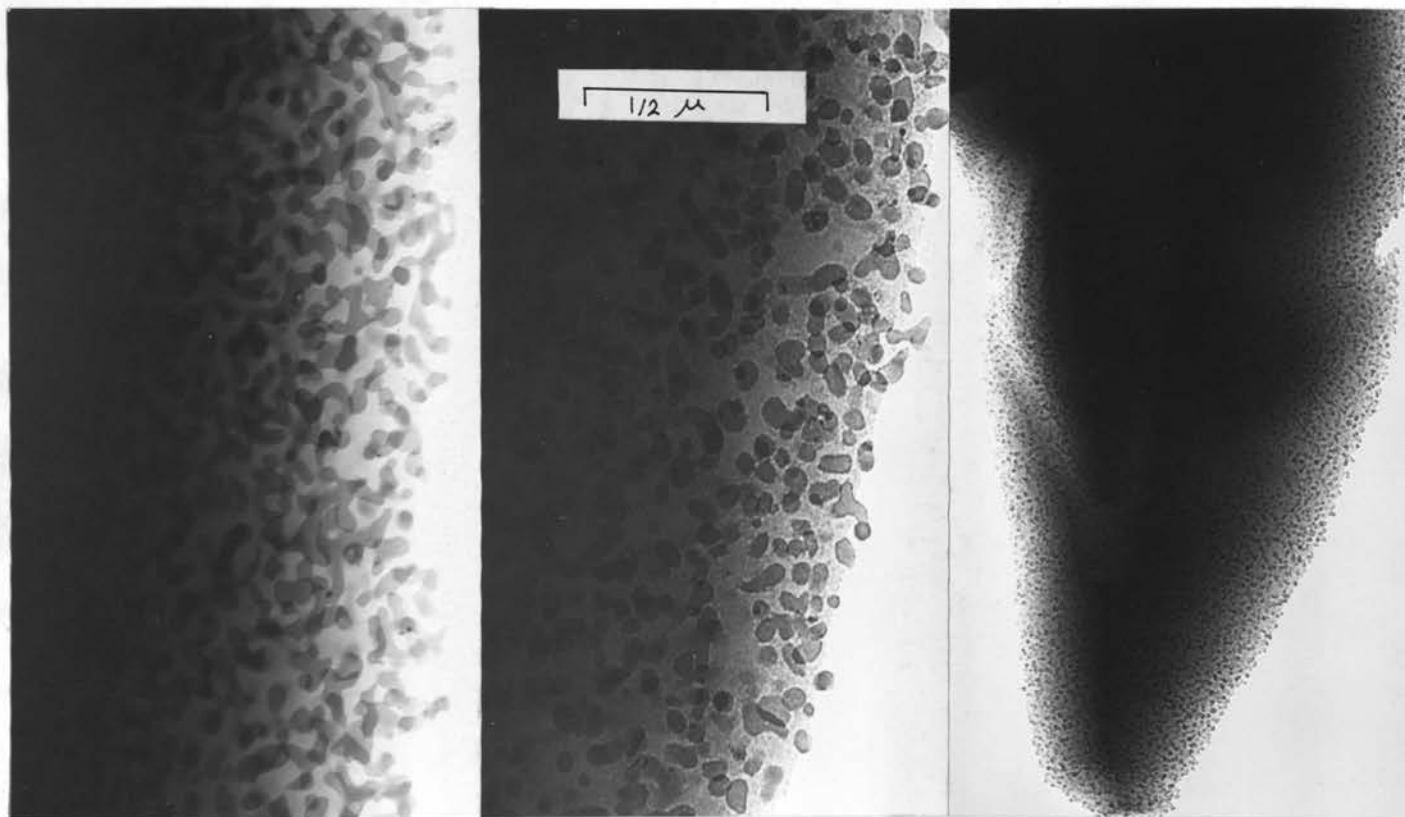
A

BASE (13 mol%Na$_2$O

B

ZnO

C

ZrO$_2$

Figure 4. Transmission electron micrographs for (A) 13 mol%Na$_2$O base glass, and 2 mol% SiO$_2$ replaced by (B) ZnO, (C) ZrO$_2$, heat treatment for one hour at 700°C.
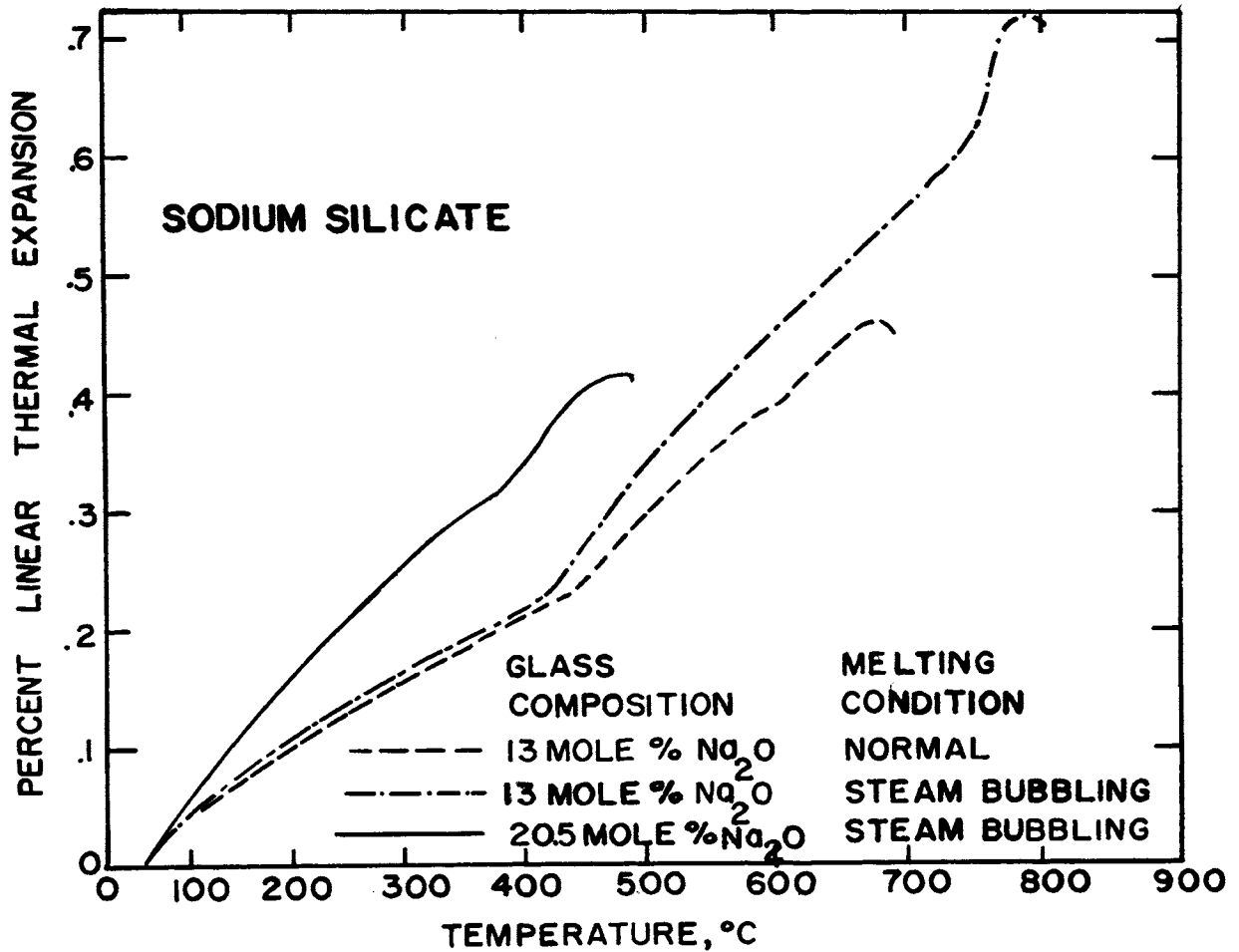
Figure 5. Expansion characteristic of glasses in the $Na_2O-SiO_2$ system and effect of OH content.

one glass temperature (Tg) is indicated by a single inflection in the curve, obviously that for the continuous soda rich-phase. The 13 mol % $Na_2O$ glass, which is in the unstable (spinodal) phase separation region and should have two interconnected phases, clearly shows two transformation temperatures (Tg), one for each phase. The effect of increasing OH content on the thermal expansion is illustrated for the 13 mol % $Na_2O$ glass. Below Tg the OH content is not significant, but above the Tg the increase in the expansion with OH content is pronounced. It is also noticed that the glass temperature (Tg), for the high silica phase, and the dilatometric softening temperature shift to higher temperatures with increasing "OH" content. Since increasing "OH" content considerably increases the rate of phase separation, the composition of the high silica phase in the glass containing more OH will be closer to the equilibrium composition. This high silica phase will have a higher Tg and softening point.

Fig. (6) shows the effect of soda content on Tg, determined from the cooling curves, for the glasses of high and low "water" content. The Tg reported here is that for the soda rich phase which can be detected in all compositions. This Tg increases steadily but slowly with increasing $SiO_2$ content. This increase reflects the degree of deviation of the soda rich phase from equilibrium composition. Increasing "water" content seems to lower the Tg of the soda rich
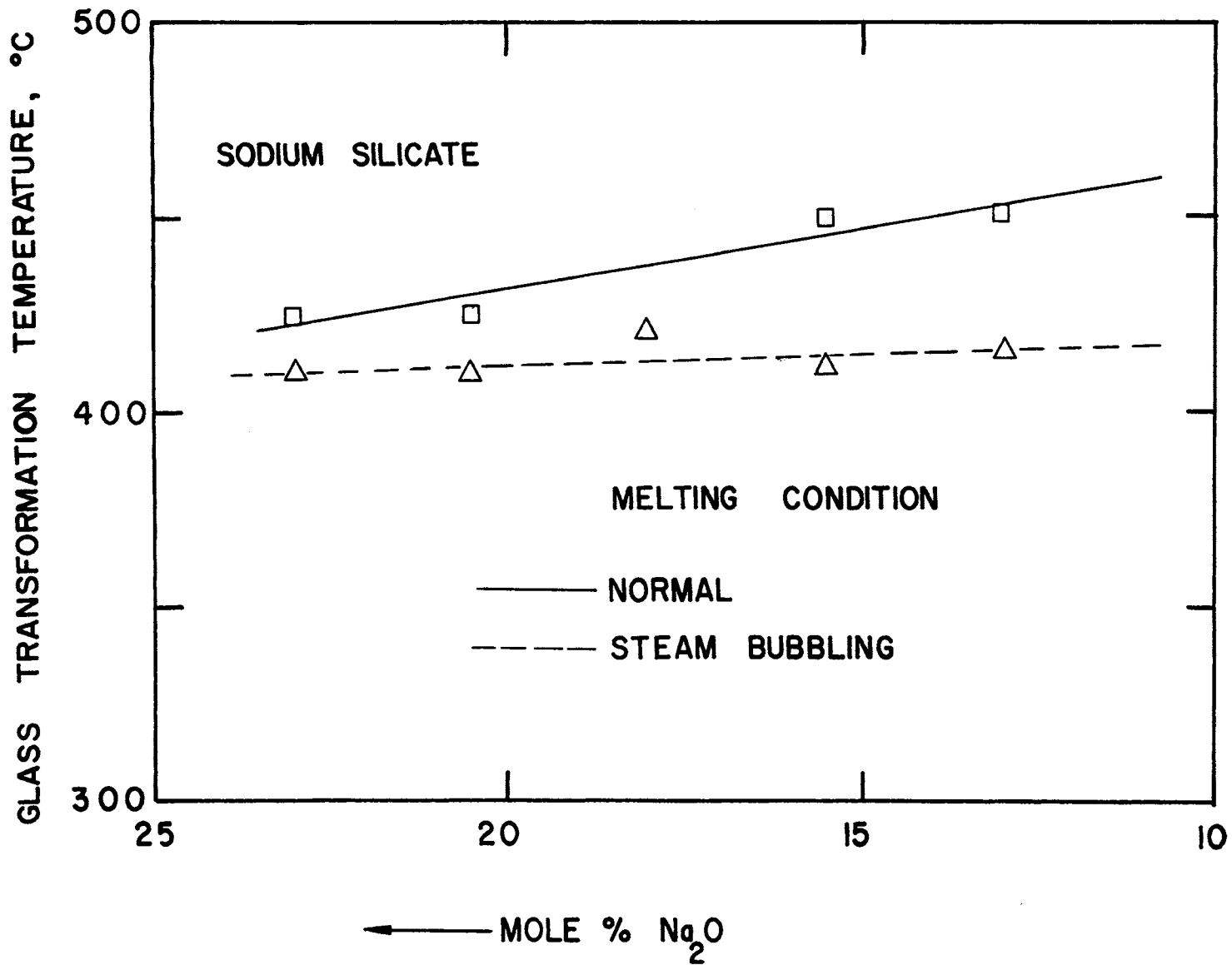
Figure 6. Effect of OH content on the glass transformation temperature in the $Na_2O$-$SiO_2$ system

phase, and the effect is more pronounced in the high silica glasses. The Tg for the high silica phase is detectable only in the high silica glasses having a high connectivity in the silica rich phase[14].

The linear coefficients of thermal expansion were determined from room temperature to 400$^\circ$C in the composition range between 23 and 13 mol % $Na_2O$ and found to increase linearly with total sodium content, in agreement with earlier studies[15]. The thermal expansion coefficients for the linear part of the curve above Tg, were calculated and plotted as a function of the $Na_2O$ content (Fig. 7). Fig. (7) shows that the coefficients do not decrease linearly with decreasing $Na_2O$ content. From 23% to 20% $Na_2O$ the coefficient decreases rapidly. From 20 to 15 mol % $Na_2O$ there is very little change, but below 15% the coefficient decreases again, however not as rapidly as above 20%. It is significant that the boundary of phase separation is generally found at about 20%[7,15,16] $Na_2O$. At this point the composition of the soda rich continuous phase is almost constant. This may account for the small change of expansivity in this range, but it would require data at different degrees of phase separation to analyze this behavior. An increase in the water content of the glass increases the expansion coefficient.

Infrared measurements had shown that all compositions melted under normal atmosphere contained about .02 and all
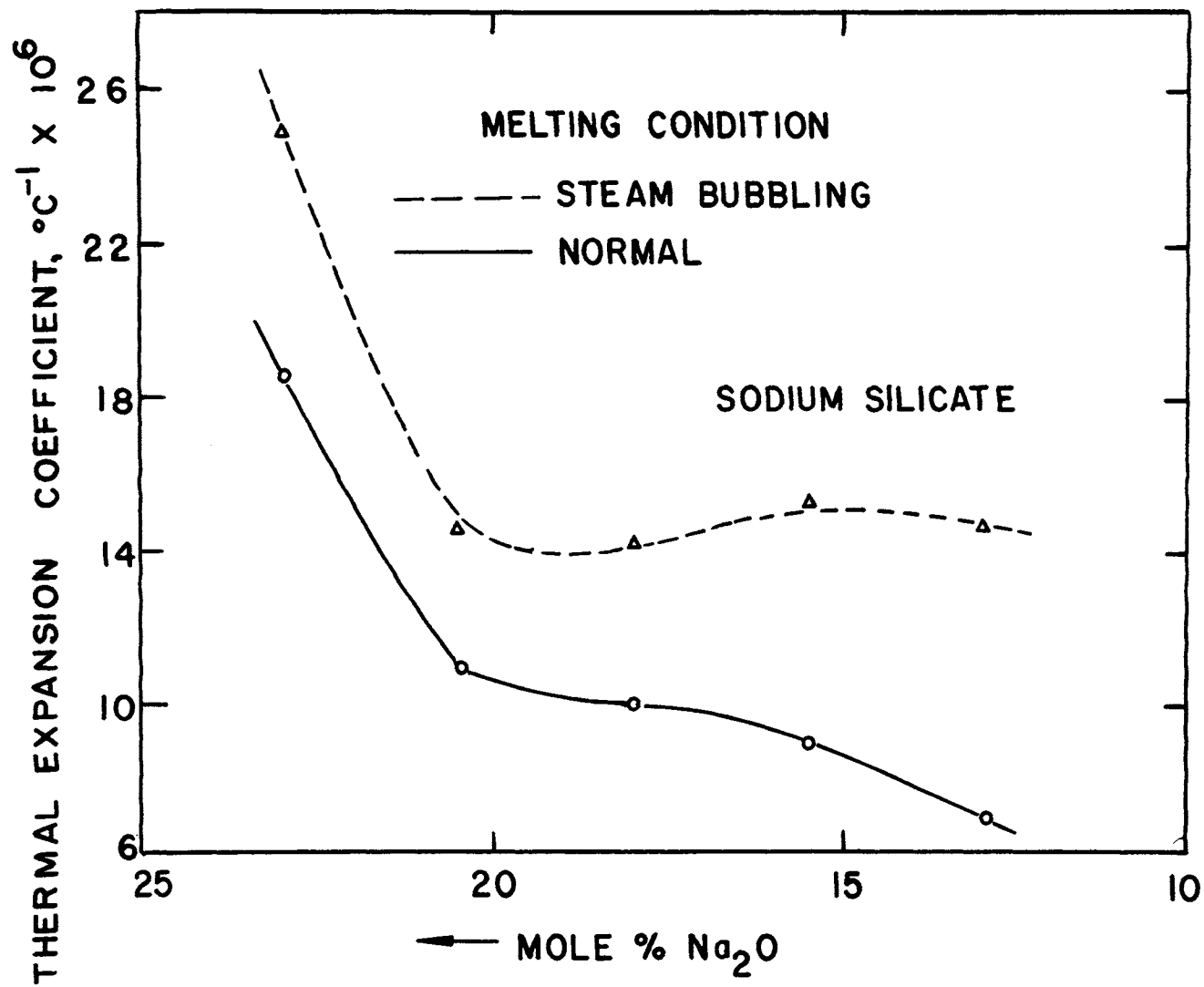
Figure 7. Effect of OH content on the variation of thermal expansion coefficient

with composition above Tg.

compositions melted with steam bubbling about .1 wt % OH.
The effect of water on increasing the expansion coefficient
was more pronounced in the high silica content glasses.
This observation could be explained by considering that
the reaction of water with the high silica continuous
phase is more effective in increasing the expansion
coefficient than that with the continuous soda rich phase,
which has a higher concentration of non-bridging oxygen
to begin with.

## 3.22 The Dilatometric Softening Temperature

The type of microstructure developed in the glass
definitely affects the dilatometric softening point[15].
The development of two interconnected phases results in an
increase in the softening temperature of the decomposed
glasses compared to that of the undecomposed glasses.
The volume percentage of the high silica phase present
and probably the interfacial stresses developed between
the two phases would influence the softening point.
Fig. (8) shows the change of the dilatometric softening
temperature with soda content for glasses with low and
high "water" content respectively. In glasses with low
"water" content there is a slight increase in the softening
temperature up to about 15 mol % $Na_2O$, then followed by a
sharp increase with further additions of $SiO_2$.
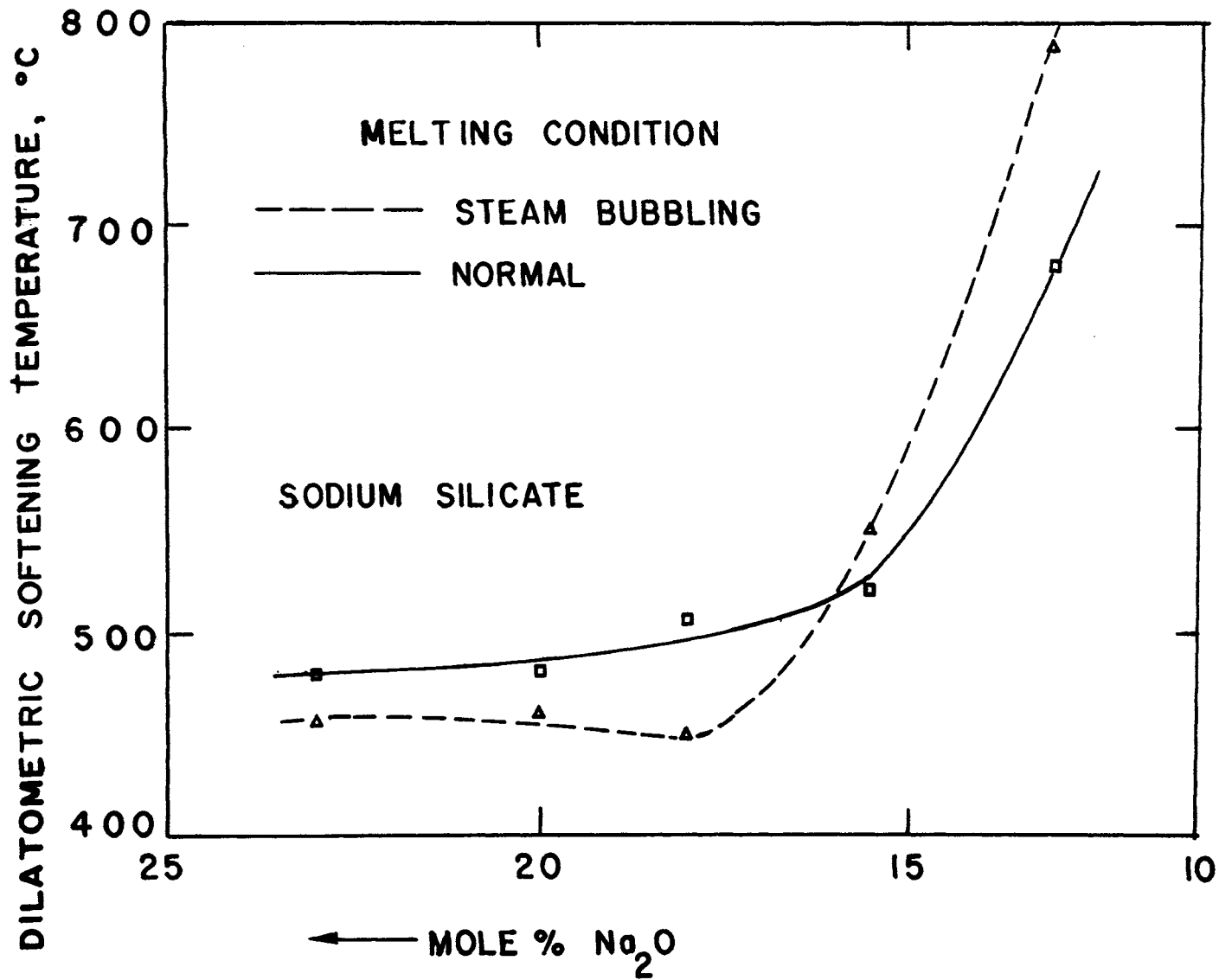
Figure 8. Effect of OH content on the dilatometric softening temperature in the $Na_2O$-$SiO_2$ system.

The glasses with high "water" content have a lower softening temperature which remains almost constant to 15 mol % $Na_2O$. Below 15 mol %, however, the softening temperature rises steeply and becomes even higher than that of the low "water" content glasses. The crossing of the curves occurs at about 15 mol %, just about where the change to the connective morphology of unstable phase separation is expected to appear. The presence of "water" in promoting the rate of separation, may shift the compositions of the separated phases closer to equilibrium: i.e., to higher $SiO_2$ content in the connected silica-rich phase below 15 mol % $Na_2O$, to higher $Na_2O$ in the continuous soda-rich phase above 15 mol %.

In summary, the increase in OH content of the glass increases its thermal expansion coefficient above Tg and changes the softening point in a direction that is determined primarily by the microstructure for the glass. Also the glass temperature of the soda rich phase shows a decrease with increase in OH content. The study of the thermal expansion coefficient above Tg and of the dilatometric softening point could be used to indicate the presence of phase separation in a glass system and help locate areas with different microstructure within the phase separation dome. Similarly, Shaw et al[45], have used density data.

## 3.3 RADIATION INDUCED OPTICAL ABSORPTION

Fig. (9) shows the effect of increasing "water" content

on the intrinsic visible and uv absorption in the 18 mol %

$Na_2O$ sodium silicate glasses. Glasses No. 1,2, and 3 were

melted under normal pressure, but glass No. 4 was melted

under vacuum. In glasses No. 1,2, and 3, the uv absorption

around 5 eV increases with the increase in the OH concentra-

tion. It was suggested[17] earlier that the uv absorption

in glass is associated with the formation of non-bridging

oxygens. It is possible that this absorption around 5 eV

is associated with hydroxyl group formation, if we consider

that the rupture of the glass network by water is similar

to, but not the same as, that caused by additions of alkali

oxide. The lowest OH content glass (No. 4) melted under

vacuum, has even higher uv absorption than other glasses.

This could be caused by the reduction of the glass during

melting under vacuum through the formation of non-bridging

oxygen vacancies. Similar observations were reported for

water free vitreous silica, which is normally produced in

a partially reduced state; it absorbs in the uv at 2425 $A^{o}$

and exhibits fluorescence[18]. Absorption as well as

fluorescence were removed, when this silica was heated

under oxidizing atmosphere, at a rate which is probably

determined by the diffusion of oxygen through the solid.

In general, it has been found that the radiation-

induced absorption spectra of alkali silicate glasses can

be resolved into four absorption bands centered at about

2.0, 2.9, 4.0, and 5.5 eV respectively. Stroud[19]
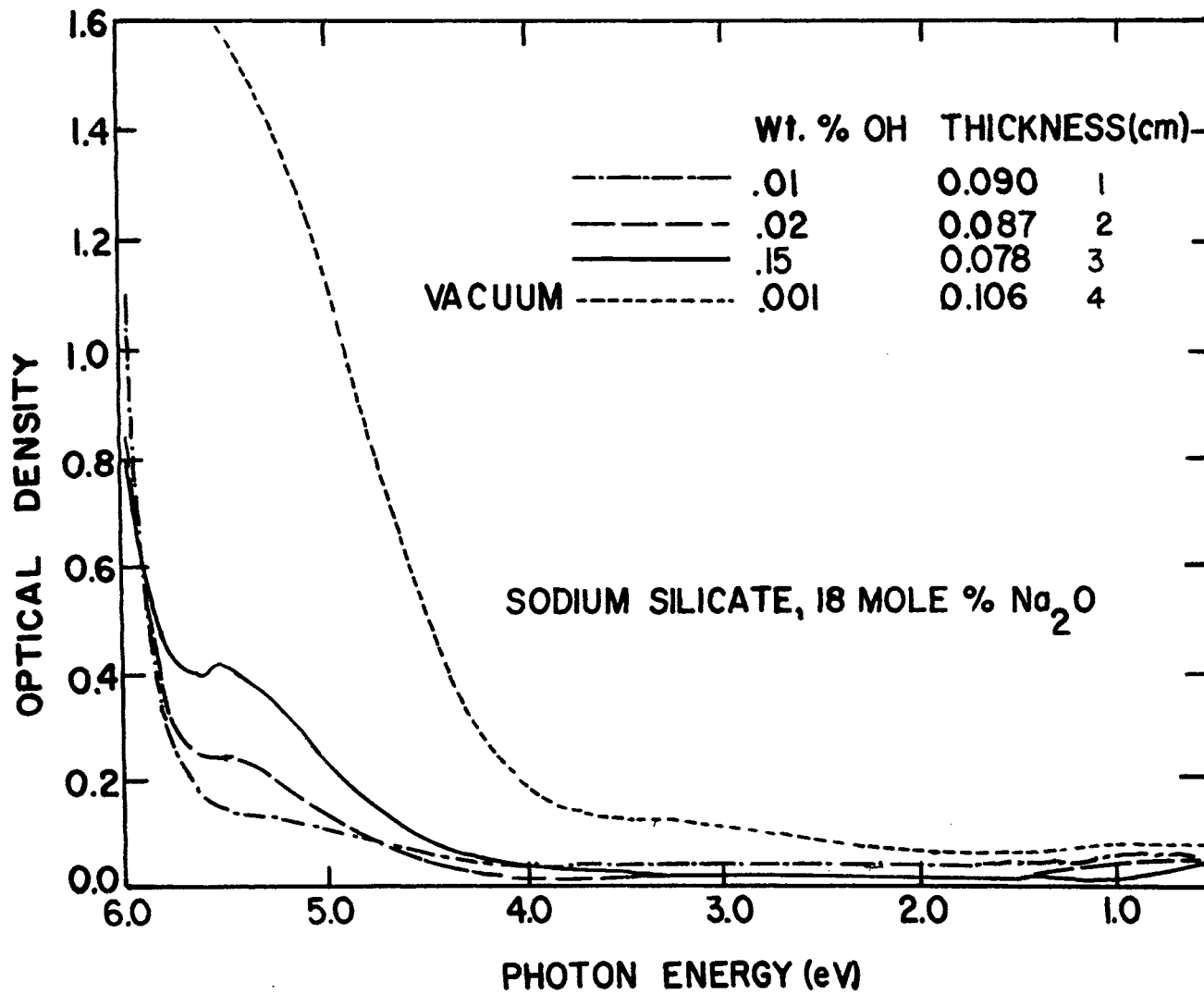
Figure 9. Effect of OH content on the intrinsic visible and uv absorption in the
18 mol % Na$_2$O glasses.

concluded, that the two induced visible absorption bands at about 2.0 and 2.9 eV are due to trapped holes. A similar conclusion has been reached by Mackey et al.[20,21] and Bishay[22]. Investigations, by Yokota[23] and later on by Kats and Stevels[24], and Bishay and Ferguson[25], suggested that the 4.0 eV induced band in silicate glasses is attributed to a positive hole trapped by an alkali vacancy neighboring an oxygen ion.

Fig. (10) shows the radiation induced optical absorption for the 18 mol % $Na_2O$ sodium silicate glasses of different OH concentration. The spectra for glasses No. (1) and (2) and (3) show an increase in the intensity of the three visible induced absorption hole centers with increasing OH content. This suggests that rupture of the glass network and formation of hydroxyl groups enhance the formation of the induced hole centers which are most probably close to non-bridging oxygens formed through the reaction of water with the silica network. On the other hand, the electron trap centers induced in the uv region beyond 4.0 eV are suppressed with increasing OH content, as shown in Fig. (11) curves (1) and (3). The formation of more non-bridging oxygen, by reaction of $H_2O$ with the glass network, could suppress the intensity of the uv induced electron trap centers by competing with these centers in capturing the electron liberated during irradiation.
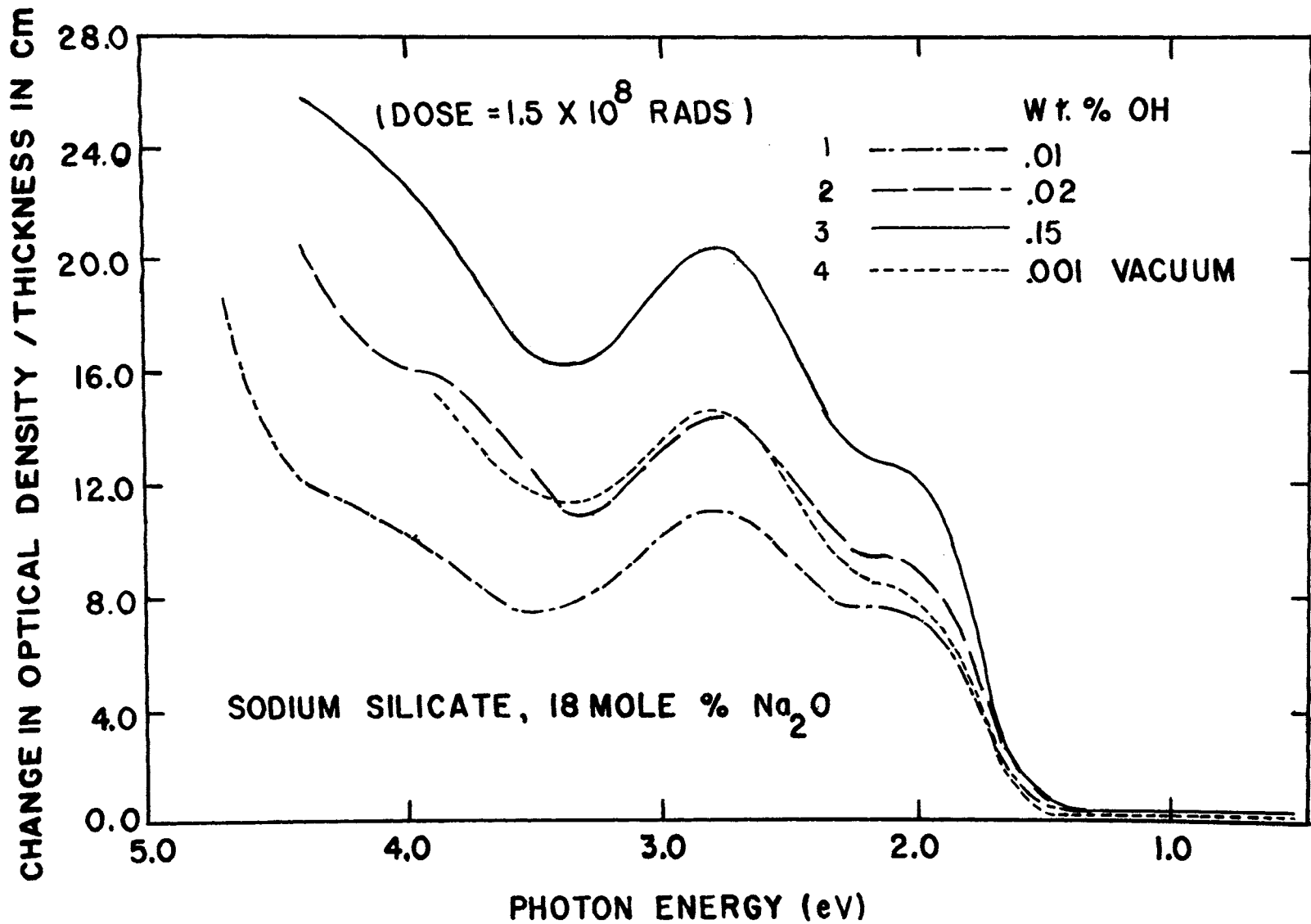
Figure 10. Effect of OH content on the x-ray induced absorption in the 18 mol % $Na_2O$ glasses.
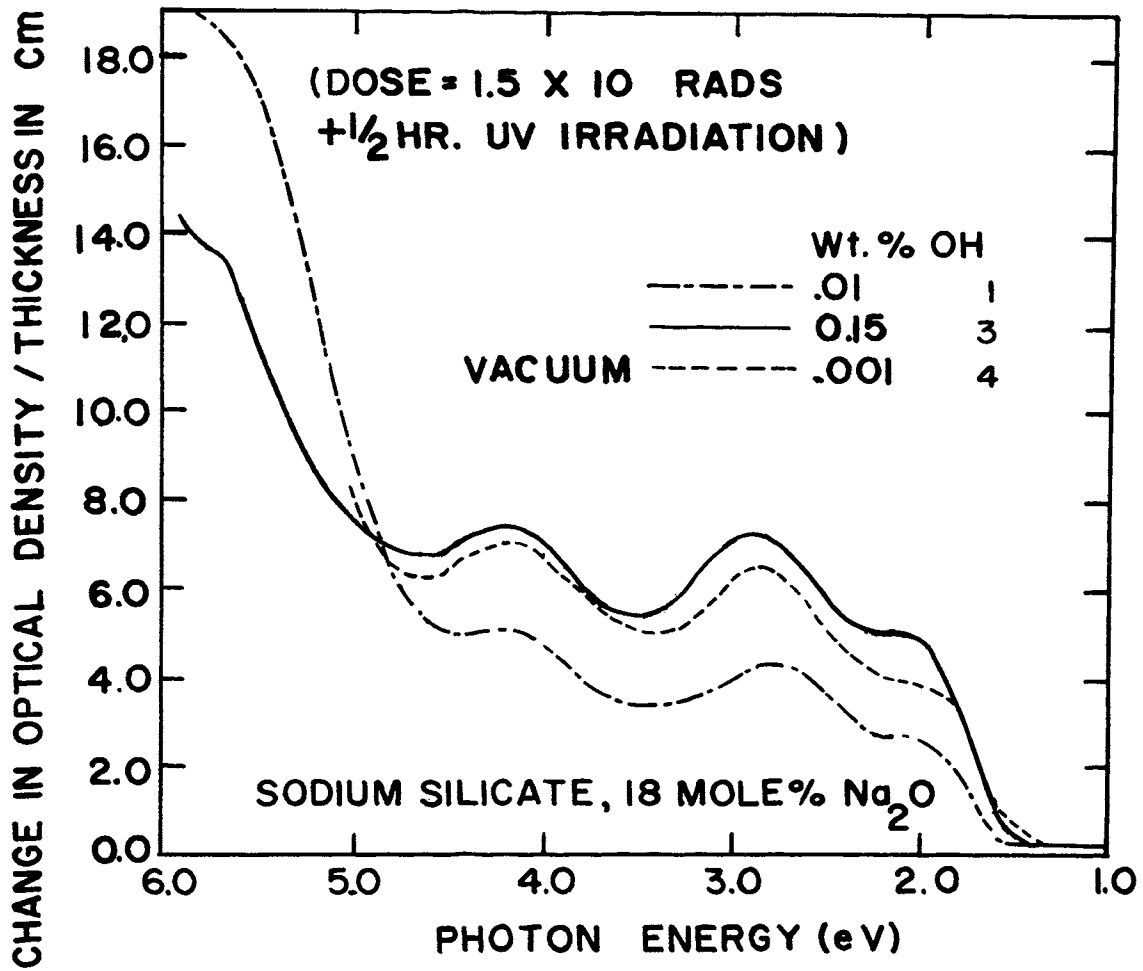
Figure 11. Effect of OH content on x-radiation induced optical

absorption in the 18 mol % $Na_2O$ glasses, after bleaching

with short wave length uv irradiation.

Glass No. 4 melted under vacuum gave a higher induced absorption than expected from its low OH content. This might be attributed to the formation of alkali vacancies capable of trapping more positive holes which might outweigh the decrease in the non-bridging oxygen. The decrease in non-bridging oxygen by melting under vacuum could be described in the following reaction: $\equiv$ Si-OH HO-Si $\equiv$ $\xrightarrow[\text{melting}]{\text{vacuum}}$ $\equiv$ Si-O-Si $\equiv$ + $H_2O$. Fig. (11) shows the induced optical absorption for glasses No. (1,3, and 4), after x-ray irradiation and subsequent bleaching with short wave length uv irradiation. Generally, the intensity is smaller if compared with that in Fig. [10] before bleaching. From the relative change in intensity with uv bleaching, it seems that the hole centers in glass No. (4), melted under vacuum, are more stable. More quantitative study on the stability of the centers in this glass is needed.

Although the change in OH concentration is insignificant in comparison with the alkali content, its effect on the induced optical absorption is substantial.

## 3.4 INTERNAL FRICTION

Two peaks are observed when measuring the internal friction as a function of temperature in alkali silicate glasses. The low temperature peak in alkali silicate glasses is attributed to the stress-induced movement of the alkali ions[26,27,28]. The mechanism for the internal

friction peak at higher temperature (200-300$^{\circ}$C) has not
been explained satisfactorily. One explanation suggests
that the loss is caused by stress induced movement of the
non-bridging oxygen ions[29,30], another explanation con-
siders that the interaction between alkali ions and
bridging proton is responsible for the effect[31,32].

Glasses containing a mixture of dissimiliar alkali
ions exhibit an unusually large internal friction peak as
first reported by Rötger[33] and Jagdt[34]. Steinkamp et
al.[35] concluded that this is a new peak and is observed
only in mixed alkali glasses. An elastic dipole model was
proposed[6] to explain this peak, where the dissimilar
alkali ions interchange their position. Recently, this
model was supported with a correlation between the height
of the mixed peak and the diffusion coefficients of the
dissimilar alkali ions[36].

Fig. (12) shows the internal friction curves for
sodium silicate glasses (18 mol % $Na_2O$) with different
water content. The low temperature alkali peak decreases
and moves to higher temperature with increasing water con-
tent, while the high temperature peak seems to increase
with increasing water content.

The decrease of the low temperature peak was observed
by de Waal[37], in sodium disilicate glasses, where $Na^+$ ions
were exchanged for protons by treatment in molten $NH_4HSO_4$.
De Waal[37] explains the decrease in the alkali peak and
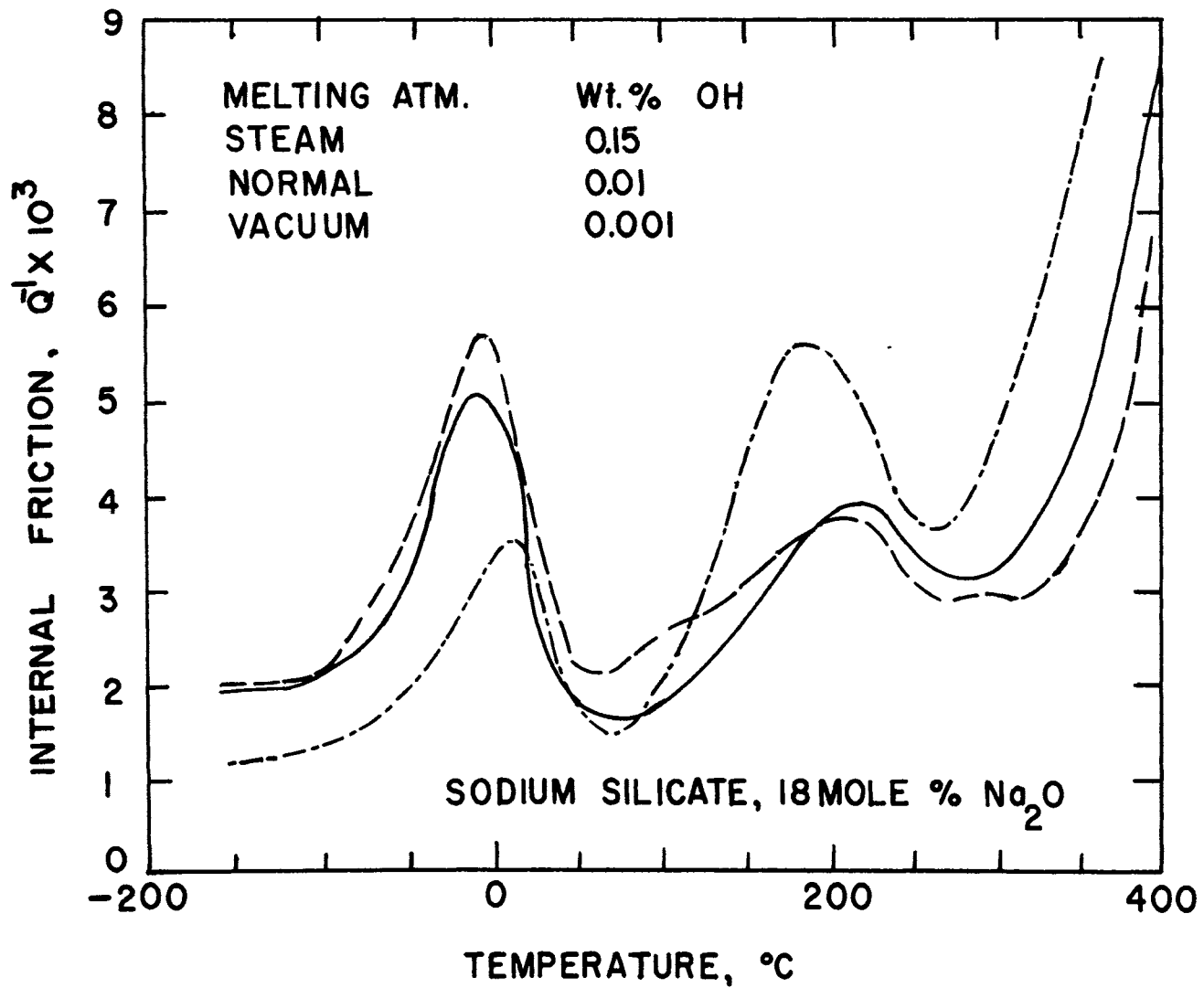
Figure 12. Effect of OH content on internal friction in the 18 mol % $Na_2O$ glasses,

Freq. = 0.4 Hz.

shifting to a higher temperature by the decrease in alkali concentration after ion exchange. This explanation is doubtful since in our experiment the alkali content is practically constant in the three glasses. We are more inclined to attribute this decrease to the similar effect observed when a second alkali was added[6,36], or introduced into the glass by ion exchange[38,39]. If we consider the correlation between the height of the alkali peak and the diffusion coefficient of alkali ions reported by McVay and Day[40], and the smaller diffusion coefficient by $Na^+$ ions in the high water content synthetic $SiO_2$ glass compared to the low OH content $SiO_2$, observed by Frischat[41], we may suggest that addition of protons, just like that of a second alkali, lower the diffusion coefficient of the principal alkali. This would lead to shifting of the peak to higher temperature and the probable amount of alkali susceptible for diffusion would be smaller, resulting in the decrease of the alkali peak height.

The high temperature peak appears to increase in size and shift to a lower temperature with OH content. Very recently Doremus[42] proposed that the high temperature internal friction peak in glass results from the stress-induced motion of hydrogen ions that are introduced by reaction of sodium ions in the glass with atmospheric water. Coenen[43] reported the absence of such a peak in soda-silica glasses melted completely free from water and

attributed this peak to the interaction of alkali ions, bridging $H^+$ ions and network ions (e.g. $O^-$). Supporting this mechanism is Revesz's[46] suggestion that the configuration

$$\equiv Si-O^- \quad \begin{matrix} H+ \\ \\ Na^+ \end{matrix} \quad {}^-O-Si \equiv$$
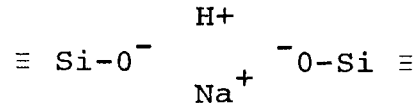
is more favorable energetically, with the possible formation of a hydrogen bond. From this configuration, one may suggest an elastic dipole model, similar to that proposed for the mixed alkali peak, and the presence of non-bridging oxygen and protons would be essential for the second peak to appear.

In brief, increasing water content in sodium silicate glasses decreases the alkali peak by decreasing the diffusion coefficient for the alkali ions, and enhances the high temperature peak by bringing more hydroxyl groups into the glass network. Since the effect is so pronounced with small changes in water content, the water content should be considered when reporting internal friction measurements.

## 4.  CONCLUSIONS

Increasing the OH content in sodium silicate glasses was found to have the following effects for the compositions indicated

(1)  enhances the phase separation kinetics

(13, 15.5 and 18 mol % $Na_2O$)

(2) decreases the glass temperature (Tg), and increases the thermal expansion coefficient above Tg; changes the softening point in a way that depends on the morphology of the microstructure (13, 15.5, 18, 20.5, and 23 mol % $Na_2O$).

(3) increases the radiation induced absorption bands associated with positive hole centers, and decreases those associated with electron trap centers (18 mol % $Na_2O$).

(4) decreases the low temperature alkali peak, and increases the high temperature peak of internal friction (18 mol % $Na_2O$).

The OH content was shown to be an important factor affecting physical properties, and should be considered and estimated when reporting data on these properties.

REFERENCES

(1)   SCHOLZE, H. Gases and water in glass.  Glass Ind.,
      4 (1966), 10, 546-51; 11, 622-28, 670-75.

(2)   KOENIG, C.J., GREEN, R.L.  Water vapor in high tem-
      perature ceramic processes.  Ohio State Univ.
      Eng. Expt. Sta. Bull. No. 202 (1967).

(3)   MARKER, L., SCHOLZE, H.  The influence of water con-
      tent of silicate glasses on their transformation
      and softening behavior.  Glastech. Ber., 35 (1962),
      1, 37-43.

(4)   GOETZ, J., VOSAHLOVA, E.  Quantitative determination
      of water content in glass with the aid of infrared
      OH bands.  Glastech. Ber., 41 (1968), 2, 47-55.

(5)   LUSK, G.R. Absolute specification of x-ray spectra by
      Laplace transform analysis of attenuation data.
      M.S. Thesis, Univ. of Missouri-Rolla (1968)

(6)   SHELBY, J.R., DAY, D.E.  Mechanical relaxation in
      mixed-alkali silicate glasses.  J. Amer. Ceram.
      Soc., 52 (1969), 4, 69-74.

(7)   TRAN, T.L.  Study of phase separation and devitrifi-
      cation products in glasses of the binary system
      $Na_2O-SiO_2$.  Glass Technol., 6 (1965), 5, 161-165.

(8)   CHARLES, R.J.  Metastable liquid immiscibility in
      alkali metal oxide-silica systems.  J. Am. Ceram.
      Soc., 49 (1966), 2, 55-62.

(9)   HALLER, W.  Rearrangement kinetics of the liquid-
      liquid immiscibility microphases in alkali
      borosilicate melts.  J. Chem. Phys., 42, (1965), 2,
      686-93.

(10)  NEILSEN, G.F.  Spinodal decomposition in soda silica
      glasses.  Phys. Chem. Glasses, 10 (1969), 2, 54-62.

(11)  HALLER, W., MACEDO, P.B.  The origin of phase connecti-
      vity in micro-heterogeneous glasses.  Phys. Chem.
      Glasses, 9 (1968) 5, 153-155.

(12)  MCCURRIE, R.A., DOUGLAS, R.W.  Diffusion-controlled
      growth of second phase particles in lithium sili-
      cate glasses.  Phys. Chem. Glasses, 8 (1967), 4,
      132-139.

(13)  MORIYA, Y., WARRINGTON, D.H., DOUGLAS, R.W.  A study
      of metastable liquid-liquid immiscibility in some
      binary and ternary alkali silicate glasses.  Phys.
      Chem. Glasses, 8 (1967), 1, 19-25.

(14)  MAZURIN, O.V., STRELTSINA, M.V., TOTESH, A.S.  The
      viscosity and transformation temperature of phase-
      separated sodium borosilicate glasses.  Phys.
      Chem. Glasses, 10 (1969) 2, 63-71.

(15)  REDWINE, R.H., FIELD, M.B.  The effect of microstructure
      on the physical properties of glasses in sodium sili-
      cate system.  J. Material Science, 3 (1968), 4,
      380-388.

(16)  (a)  COOK, H.E., HILLIARD, J.E.  A simple method of
           estimating chemical spinodal.  Tran. Metallurgical
           Soc. AIME, 233 (1965), 142-46.
      (b)  ANDRE, N.S., AVERYANOV, N.J., PORAI-KOSHITS, E.A.
           Structural transformation in glass at high
           temperatures.  The Structure of Glass, Vol. 5,
           Translation Consultant Bureau, New York (1965).

(17)  STEVELS, J.M.  Note on the ultraviolet transmissivity
      of glass.  Proceedings of the XI Congress on Pure
      and Applied Chemistry, 5 (1947),5, 519-521.

(18)  BELL, T., HETHERINGTON, G., JACK, K.H.  Water in
      vitreous silica, Part 2:  Some aspects of hydrogen
      water-silica equilibria.  Phys. Chem. Glasses, 3
      (1962), 5, 141-146.

(19)  STROUD, J.S.  Color centers in a cerium-containing
      silicate glass.  J. Chem. Phys., 37 (1962),
      4, 836-841.

(20)  MACKEY, J.H., SMITH, H.L., HALPERIN, A.  Optical
      studies in x-irradiated high purity sodium silicate
      glasses.  J. Phys. Chem. Solids, 27, (1966) 11/12,
      1759-72.

(21)  MACKEY, J.H. SMITH, H.L., NAHUM, J.  Ccompetitive
      trapping in sodium disilicate glasses doped with
      $Eu^{+3}$.  J. Phys. Chem. Solids, 27 (1966) 11/12,
      1773-82.

(22)  BISHAY, A.  Radiation induced color centers in multi-
      component glasses.  J. Non-Cryst. Solid, 3 (1970),
      1, 54-114.

(23)  YOKOTA, R.  Color centers in alkali silicate and borate
      glasses.  Phys. Rev. 95 (1954), 1145-48.

(24) KATS, A., STEVELS, M. The effect of uv and x-ray
     radiation on silicate glasses, fused silica and
     quartz crystals. Philips Res. Rept. 11 (1956),
     115-156.

(25) BISHAY, A., FERGUSON, K.R. Gamma-ray-induced coloring
     of glasses in relation to structure. Advanced in
     Glass Tech. Proc. VI Intern. Congr. on Glass,
     Washington, 1962 (Plenum Press, New York)p. 133.

(26) FITZGERALD, J.V. Anelasticity of glasses. J. Amer.
     Ceram. Soc. 34 (1951), 11, 339-44.

(27) RÖTGER, H. Elastic after effect from thermal diffu-
     sion and matter diffusion by periodic and aperiodic
     methods. J. Amer. Ceram. Soc., 19 (1941), 6,
     192-200.

(28) MOHYUDDIN, I., DOUGLAS, R.W. Observation of the
     anelasticity of glasses. Phys. Chem. Glasses,
     1 (1960), 3, 71-86.

(29) RYDER, R.J., RINDONE, G.E. Internal friction of simple
     alkali silicate glasses containing alkaline-earth
     oxide. J. Amer. Ceram. Soc., 44 (1961), 11,
     532-40.

(30) DAY, E.E., RINDONE, G.E. Properties of soda alumino-
     silicate glasses. J. Amer. Ceram. Soc. 45 (1962),
     10, 496-504.

(31) COENEN, M. Mechanical relaxation of silicate glasses
     with eutectic composition. Z. Electrochem., 65
     (1961), 10, 903-908.

(32) BRUCKNER, R. Characteristic physical properties of
     the chief oxide glass formers and their relation
     to the structure of glass. Glastech. Ber., 37
     (1964), 12, 536-48.

(33) RÖTGER, H. Elastic relaxation behavior of single and
     mixed alkali silicates and borates. Glastech.
     Ber., 31 (1958), 2, 54-60.

(34) JAGDT, R. Studies of relaxation phenomena in alkali
     silicate glasses. Glastech. Ber., 33 (1960),
     1, 10-19.

(35) STEINKAMP, W.E., SHELBY, J.E., DAY, D.E. Internal
     friction of mixed-alkali silicate glasses. J.
     Amer. Ceram. Soc., 50, (1967),5, 271.

(36) MCVAY, G.L., DAY, D.E.   Diffusion and internal friction in Na-Rb silicate glasses.  J. Amer. Ceram. Soc., 53 (1970) 9, 508-518.

(37) de WAAL, H.   Influence of proton exchange on internal friction in alkali silicate glasses.  J. Amer. Ceram. Soc. 52 (1969) 3, 165-166.

(38) de WAAL, H.   Internal friction in ion-exchanged sodium silicate glasses and in aluminoborate glasses. Ph.D. Thesis, Delf Technical Univ., Delf Holland, 1961, 140.

(39) de WAAL, H.   Internal friction of sodium disilicate glass after ion exchange.  Phys. Chem. Glasses, 10 (1969),3, 108-116.

(40) MCVAY, G.L., DAY, D.E.   Diffusion and internal friction in single alkali glasses.  J. Amer. Ceram. Soc., 53 (1970) 5, 284.

(41) FRISCHAT, G.H.   Mobility of sodium ion in synthetic $SiO_2$ glass.  Zeitschrift fuer Angewandte  Physik, 25 (1968, 3, 163-166.

(42) DOREMUS, R.H.   Weathering and internal friction in glass, J. Non-Cryst. Solids, 3, (1970), 4, 369-374.

(43) COENEN, M.   Influence of anisotropic on the relaxation of silicate glasses and general systematic of damping mamima in glasses.  Physics of Non-Cryst. Solids, Proceedings of the International Conference, Delft,July (1964), pp. 445-60.

(44) MARTINSEN, W.E., MCGEE, T.D.   Effects of water retention on selected properties of soda-silica glasses, Presented at the 72nd Annual Meeting of the Amer. Ceram. Soc. May 1970.

(45) SHAW, R.R., UHLMANN, D.R.   Effect of phase separation on the properties of simple glasses, I: density and molar volume, J. Non-cryst. Solids, 1 (1969), 6, 474-498.

(46) DOREMUS, R.H.   The diffusion of water in fused silica. "Reactivity of Solids", Proceedings of the VIth International Symposium on Reactivity of Solids, WILEY-INTERSCIENCE (1968), p. 673.

## VITA

Mokhtar Sayed Maklad was born on February 25, 1941, in Assyout, Egypt. He has received his college education from Ain-Shams University in Cairo; Cairo University, in Cairo; and the University of Missouri-Rolla, in Rolla, Missouri. He received a Bachelor of Science Degree in Physics and Chemistry from Ain-Shams University, in Cairo, Egypt in June 1962, a diploma in Radiation Physics from the same University, in April 1964, and a Master of Science Degree in Physics from Cairo University, in Cairo, in April 1967.

He has been enrolled in the Graduate School of the University of Missouri-Rolla since October 1967 and has held the Materials Research Assistanceship from the period October 1967 to December 1970.

APPENDICES

APPENDIX A

### Effect of Water Content on the Phase Separation in Soda Silica Glasses

Water dissolves chemically in glass and its effect on glass properties has been reviewed by Scholze[1] and Koening and Green[2]. Solution is considered to occur through the formation of OH groups. This solubility has been found to be proportional to the square root of the water vapor partial pressure[1]. The following reaction describes the process of solution:

$$\equiv Si-O-Si \equiv +H_2O \rightarrow 2 \equiv SiOH$$
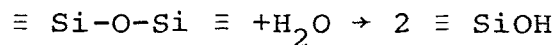
The rupture of the strong Si-O-Si bond suggest a decrease in the viscosity and surface tension with increasing water vapor partial pressure. This decrease has been verified[3].

The purpose of the present investigation was to study the effect of water vapor on the kinetics of phase separation in soda silica glasses in which the rate of separation of phases can be followed experimentally with relative ease.

A soda silica glass (18wt% $Na_2O$) was prepared by melting reagent grade chemicals in a 100 ml. platinum crucible in an electric furnace at 1450°C. The glass was

crushed and remelted in a Mo heated controlled atmosphere furnace. One part of the glass powder was melted under normal atmosphere, while 3 psi steam pressure was maintained over another part.

The amount of water in both glasses was monitored using IR spectrophotometry as described by Goetz and Vosahsova,[4] who found Beers-Lambert law applicable and calculated the extinction coefficients. The weight percent later was calculated to be 0.038 and 0.122 for the glasses melted under normal atmosphere and steam atmosphere respectively indicating that the latter contained about three times the amount of water.

Both samples were heat-treated at $600^\circ$C controlled within $1^\circ$C for 0.75, 3, and 13 hours. The progress of phase separation was followed by transmission electron microscopy. The technique is similar to that described by Shaw and Uhlmann.[8] A thin glass flake was chipped off with a diamond file, etched for 20 seconds in 2% HF, and 30 seconds in 20% HCl, then rinsed in distilled water. The thin edges of the flake were examined under the electron microscope at a magnification of about 20,000X.

The electron micrographs obtained after the above mentioned heat treatment are shown in Figure (1). In the glass melted under normal atmosphere, isolated spheres of a silica rich phase appeared in 45 minutes. After further heat treatments, these spheres coalesced forming bigger
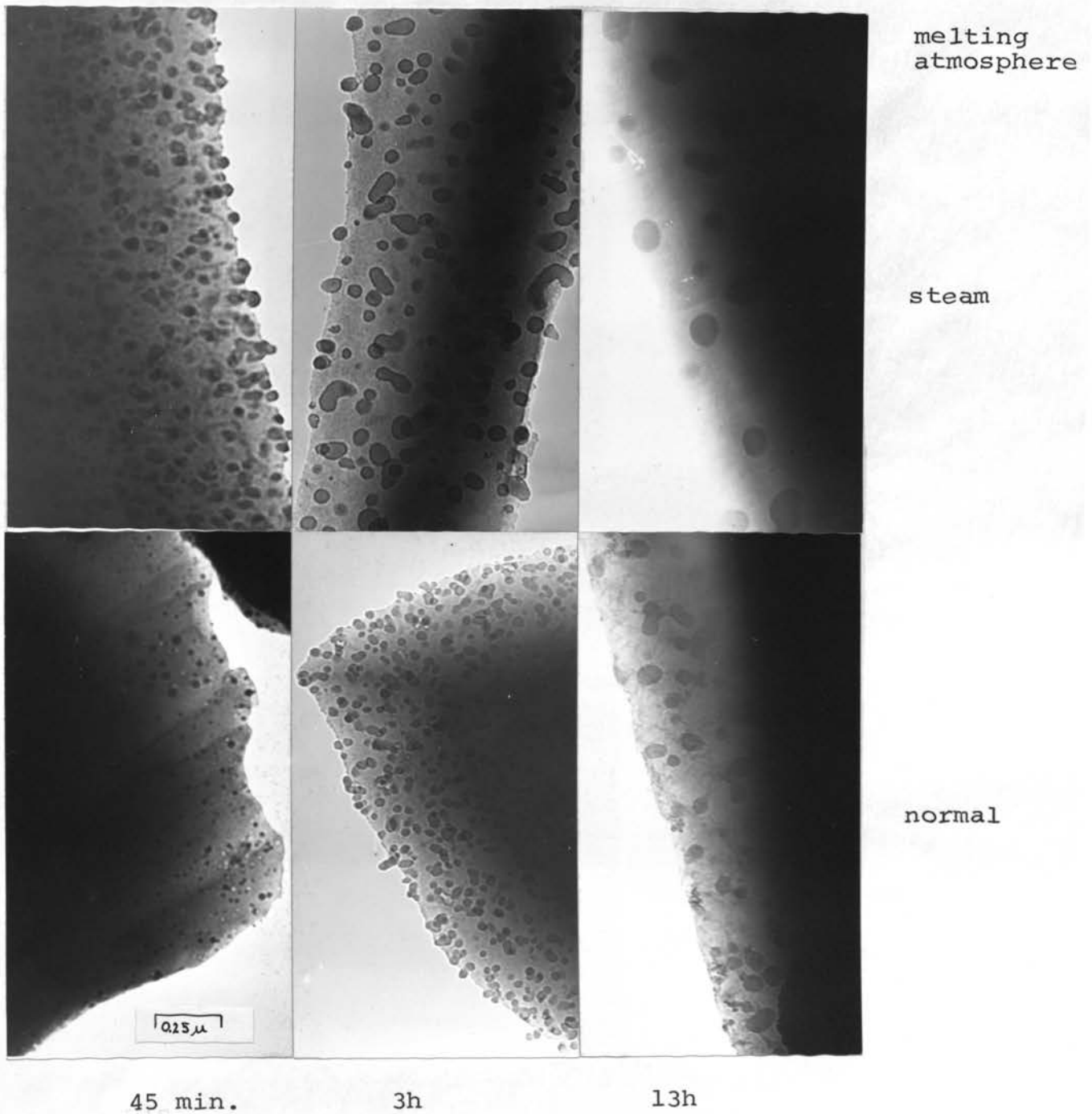
Figure 1. Electron micrographs of a soda-silica glass (18 wt % Na$_2$O heat treated at 600$^o$C; upper photos in steam atmosphere and lower photos in normal atmosphere.

droplets, with a decrease in the number of droplets per unit area. The samples melted under steam show an advanced stage of coalescence after 45 minutes treatment, indicating a faster rate of separation.

It was found also that the cube of the average particle radius increases in proportion to the time of heat treatment in both cases, as shown in Figure (2). Similar observation by Haller,[5] and reasoning by Haller and others[5,7] and Greenwood[6] suggest this variation is consistent with surface diffusion or diffusion between separated spheres as the rate controlling process. Also a variation of the slope of the curve with water content indicates the sensitivity of phase separation kinetics to small changes in the water content of the glass. In phase separation experiments, the water content of the glass must be determined and considered as an important parameter in the kinetics of the process.

The effects of replacement of small amounts of $SiO_2$ by other metal-oxides, known to assume tetrahedral coordination in the glass network e.g. $Al_2O_3$, $ZnO$ and $B_2O_3$, and conducive[9] to hinder phase separation, are currently being conducted. Also the effect of such additions on the kinetics of phase separation in soda silica glasses will be considered.
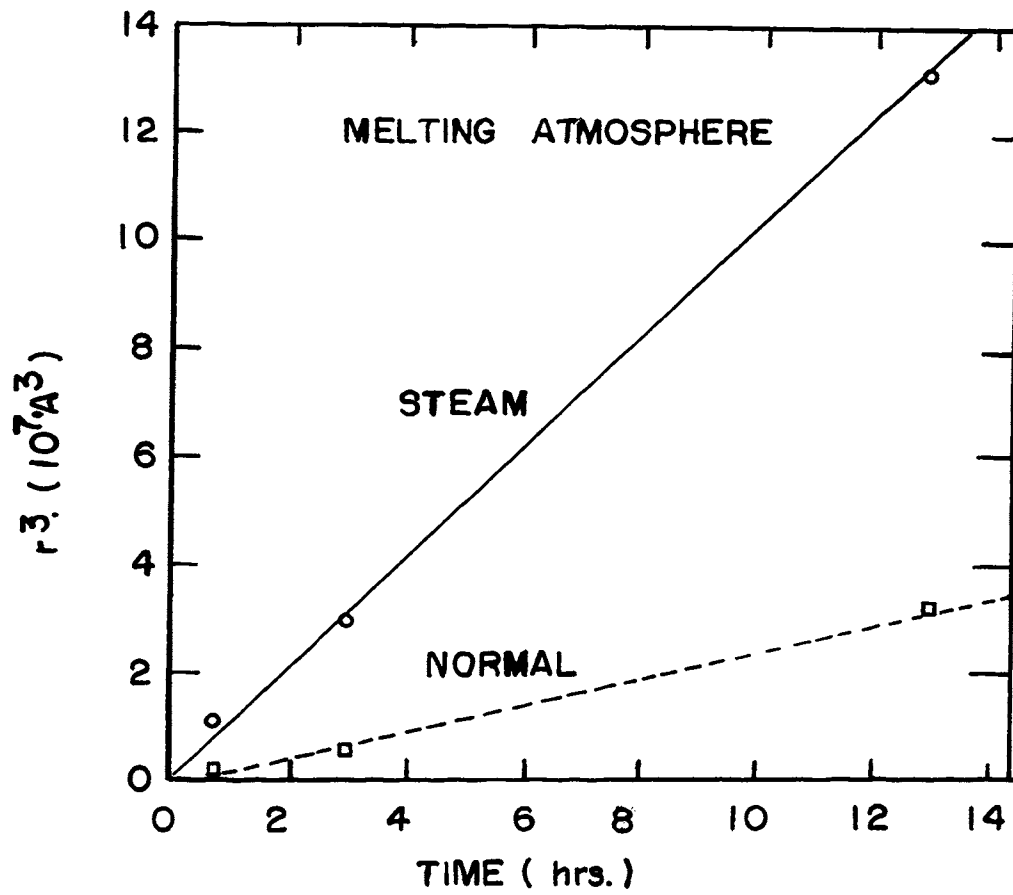
Figure 2. Effect of melting in steam atmosphere on the radial growth rate of the dispersed phase in soda-silica glasses at 600 C.

REFERENCES FOR APPENDIX A

1. Horst Scholze. "Gases and Water in Glass: I", Glass Ind. 47 [10] 435-51 (1966). "II", ibid, [11], 622-28. "III", ibid, [12] 670-75.

2. G.J. Koening and R.L. Green. "Water Vapor in High Temperature Ceramic Processes", Ohio State Univ. Eng. Expt. Sta. Bull. No. 202,(1967).

3. N.M. Parikh. "Effect of Atmosphere on Surface Tension of Glass", J. Am. Ceram. Soc. 41, [1] 18-22 (1958).

4. J. Goetz and E. Vosah'sova, "Quantitative Determination of Water Content in Glass with the Aid of Infrared OH Bands," Glastech. Ber. 41 (2) 47-55 (1968).

5. W. Haller. "Rearrangement Kinetics of the Liquid-Liquid Immiscibility Microphases in Alkali Borosilicate Melts", J. Chem. Phys. 42 686 (1965).

6. G.W. Greenwood. "Growth of Dispersed Particles in Solutions" Acta Metall. 4, (2) 243 (1956).

7. W. Haller and P.B. Macedo, "The Origin of Phase Connectivity in Microheterogeneous Glass" Phys. Chem. Glass 9 (5) (1968) 141.

8. R.R. Shaw and D.R. Uhlmann. "Subliquidus Immiscibility in Binary Alkali Borates" J. Am. Ceram. Soc. 51 [7] 377-82, (1968).

9. I. Hager, M. Hahnert and W. Hinz. "Phase Separation in Glasses of the Sodium Oxide - Silicon Dioxide Boron Oxide and Sodium Oxide - Silicon Dioxide - Aluminum Oxide System," Silikattechnik 18 (11) 360 (1967).

APPENDIX B

Glass Preparation

The glass described in Appendix A (18 wt.%$Na_2O$)
was prepared by melting under 3 psi steam pressure. A
diagram for the furnace used for melting is shown in
Fig. (1). The crushed glass was charged into a platinum
lined alumina crucible. The crucible was inserted into
the hot zone using a lowering device. The furnace was
heated with a Mo heating element. Before the crucible was
introduced into the hot zone the furnace was evacuated and
steam was introduced slowly until 3 psi steam pressure was
obtained. The water accumulated from condensation on the
cold parts, was drained continuously. At the completion
of melting, the crucible was quenched by lowering it into
the water cooled extension.

After several meltings, it was noticed that the alumina
tube of the furnace became porous and allowed the hydrogen
used to protect the heating element to get into the melting
chamber. Subsequently, another furnace having the features
of the furnace described above but heated up to $1550^{O}C$
with silicon carbide elements, was constructed. This fur-
nace was used for melting under vacuum as described earlier
in the thesis, and can be used for glass melting under steam
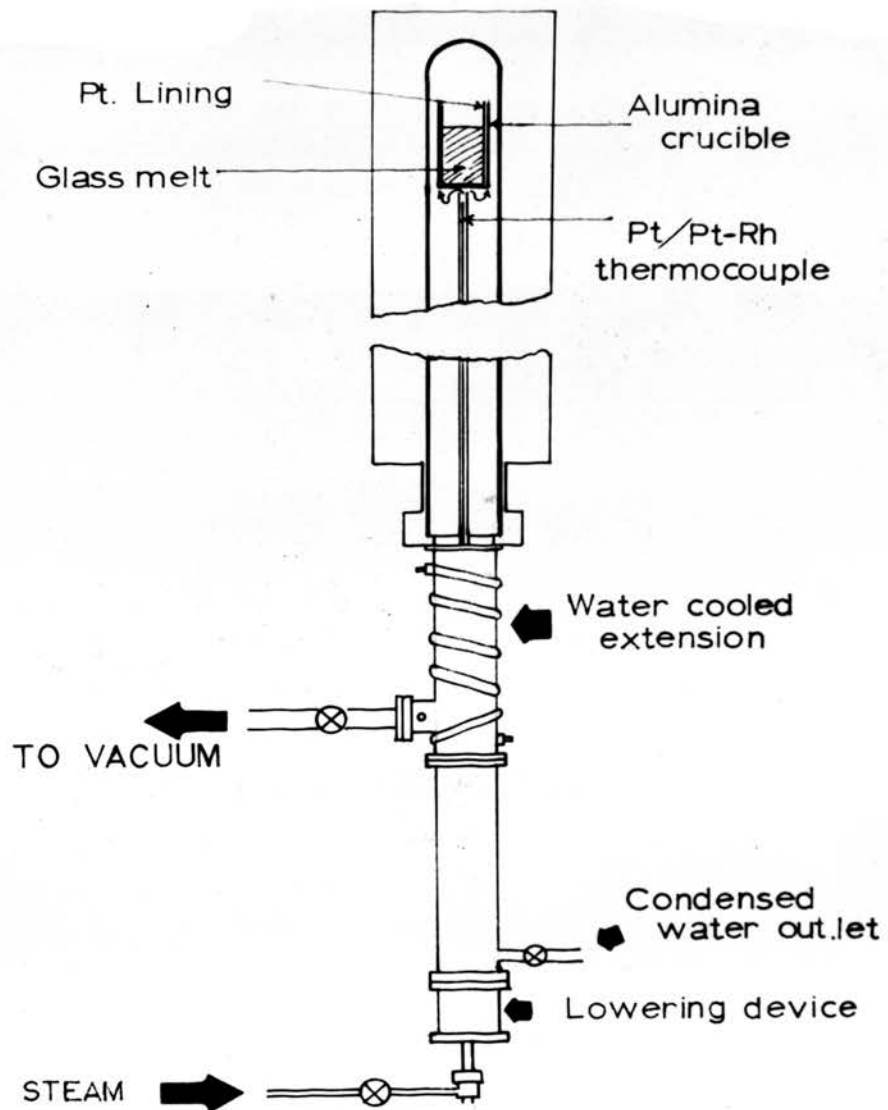pressure without the interference of hydrogen during melting.

Figure 1. Diagram of the furnace used for melting glass under steam pressure

In the case when melting under normal atmosphere, the melt was stirred with a platinum stirrer at a speed of 18 r.p.m., for 7 hours.

APPENDIX C

Electron Microscopy

1.   Sample Preparation

Transmission and replica techniques have been used in examining glasses in this study.

1.1   Transmission Technique

The glass to be examined was filled with a square 100 grit diamond file.  Tiny glass flakes in the filing were picked up with a sharp pointed pair of tweezers.  To enhance contrast, the resulting flake was etched subsequently for 20 sec. in 5% HF acid and for 10 sec. in 20% hydrochloric acid, the specimen was agitated during the acid treatment, rinsed in distilled water, and then dried with a blast of clean compressed Freon.  The flake was then, centered between two 75 mesh copper grids for observation under the electron microscope.  The flake edges were scanned for areas thin enough to transmit electrons for observation on the microscope screen.

1.2   Replica Technique

The fresh fractured surface of the glass was etched in 5% HF for 5 sec..  To remove any etch products adhering to the specimen, it was washed in 20% HCl for 20 sec., then rinsed in distilled water and dried with a clean

compressed Freon blast. The sample was placed in the evaporator for shadowing. The horizontal distance from the sample to the electrode was about 6 cm, the vertical about 3 cm. Simultaneous shadowing of 90% Pt. 10% Ir alloy and carbon was similar to the method reported by Vogel[1]. A schematic diagram for the electrode assembly is shown in Fig. (1). One end of one of the two electrodes was machined to a diameter of 2.5 mm over a length of 1 cm and a 1.2 mm hole was drilled across the electrode diameter. An N shape Pt. Ir 10% alloy wire, 1.7 mm long and 0.5 mm diameter, was inserted into the hole; a notch was made close to the hole to increase the resistance and conse-quently the temperature around the wire. This method has the advantage that the Pt. Ir alloy and carbon will be evaporated from almost a point source, and thus would increase sharpness in the resulting replica. Also shadowing with heavy metals improves the contrast of the shadowing. Evaporation was carried out at pressure $10^{-6}$ m$\mu$ and fila-ment current ranges from 40 to 50 amperes were applied to obtain a replica of desired thickness. The replica was "stripped" by slowly lowering the specimen into water at an obtuse angle. The replica floats freely onto the water. Frequently it is necessary to release the edge by begin-ning this stripping in hydrochloric or even hydrofluoric acid. If much HF acid treatment is needed, the replica is floated on HF acid for 5 minutes  to remove adhering
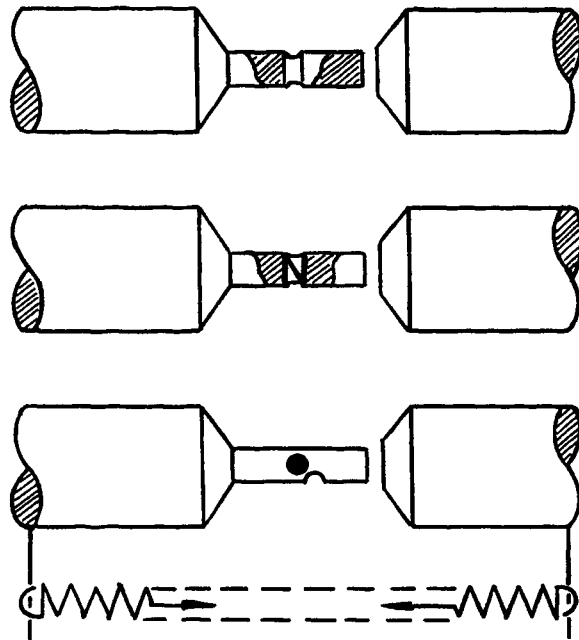
Figure 1. A schematic of electrode arrangments for the preparation of Pt Ir- C mixed layer replica. The Pt. Ir wire is placed in the drill hole of the smaller diameter part of the electrode.[1]

(etch) reaction products which otherwise show up as black spots observable in the electron microscope. The replica is then floated on distilled water for about half an hour. Replicas were picked up on copper grids to be examined under the electron microscope.

Fig. (2) shows electron micrographs for the 15.5 mol % glasses with different water content, heat treated at 700°C for 3 hours and prepared by replica and transmission techniques. Because transmission technique gave sharper micrographs and projection of real particle size, this technique was used for this study.

## 2. The Electron Microscope

For transmission electron microscopic examination of the glass samples a Hitachi HU-11A Electron Microscope was utilized. A 100-kv voltage was used to provide maximum specimen penetration and a vacuum better than $10^{-5}$ mm Hg was maintained in the microscope column. The resolution of this microscope is about 6 A°, and maximum magnification is around 300,000 X.

The microscope column, Fig. (3), is divided into three main systems. The illuminating system is composed of the electron gun which provides the electron beam, and a double condenser lense which focuses the electron beam down to a 2 micron square on the specimen. This small spot is necessary to minimize heat effects and contamination.
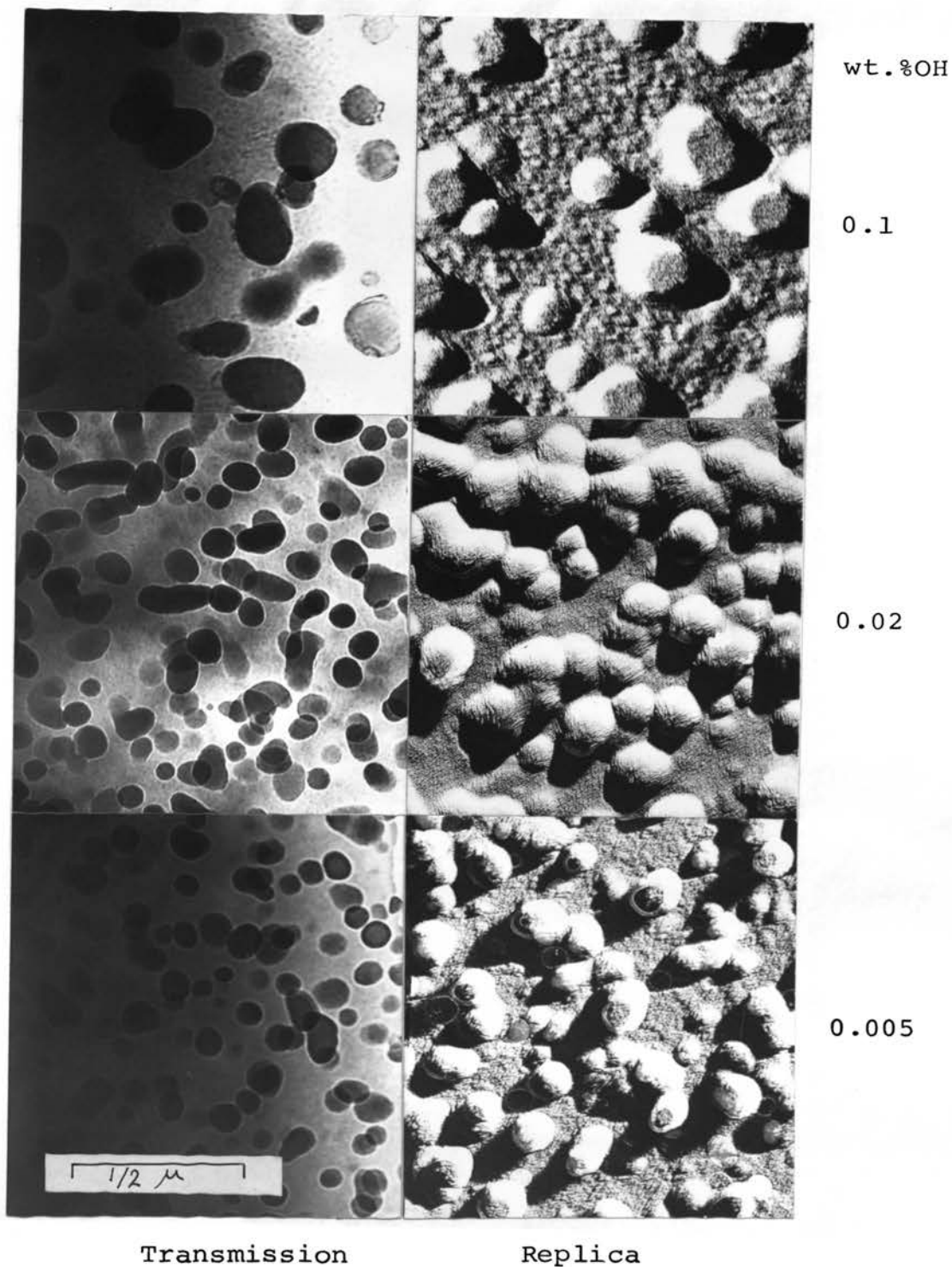
Transmission                    Replica

Figure 2.    Comparison between transmission and replica
             micrographs for 15.5 mol%Na$_2$O glass, with dif-
             ferent OH content, heat treated at 700°C for
             130 minutes.

CABLE HEAD

ELECTRON GUN

ANODE

FIRST CONDENSER LENS

SECOND CONDENSER LENS

CONDENSER APERTURE
HOLDER

SPECIMEN CHAMBER

OBJECTIVE APERTURE
HOLDER

OBJECTIVE LENS

FIELD LIMITING
APERTURE HOLDER

INTERMEDIATE LENS

DIFFRACTION SPECIMEN
CHAMBER

TURRET CONTROL KNOB

PROJECTION LENS

KNOB FOR SPECIMEN
STAGE CONTROL

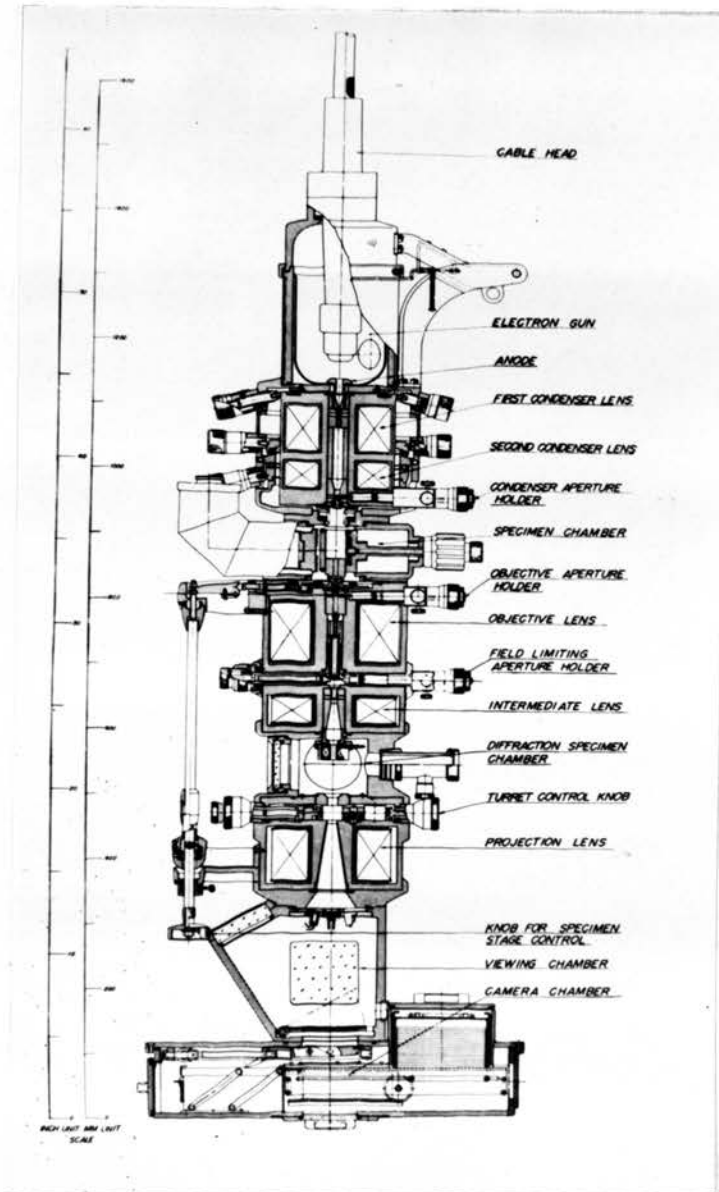VIEWING CHAMBER

CAMERA CHAMBER

INCH UNIT MM UNIT
SCALE

Figure 3. Sectional diagram of microscope
column

The image-forming system consists of the objective, intermediate and projection lenses. These three magnetic lenses provide a three stage magnification in which a change in lens current varies their focal lengths. The third system is the viewing system and consists of a viewing chamber, camera chamber, and exposure meter. The viewing chamber contains a fluorescent screen on which an image is produced by the transmitted electron beam. By raising the fluorescent screen, a film plate is exposed, providing a record of the image. An automatic exposure meter, utilizing a CdS cell as a light detector, furnishes a correct automatic exposure for a wide density variation of the illuminating beam.

Two molybdenum apertures are used in the column, one above and one below the specimen. They have the function of removing stray electrons, and of extracting, from the specimen, that part of the beam that is needed. An 0.3 mm aperture  of the second condenser lens was used to introduce onto the specimen electrons having uniform speed. The 30-micron aperture of the objective lens was used to improve contrast by eliminating the elastically scattered electrons, thus allowing only the direct beam and any low angle inelastically scattered electrons to reach the final image.

The calibration of the electron microscope was accomplished with a carbon replica of a ruled grating.
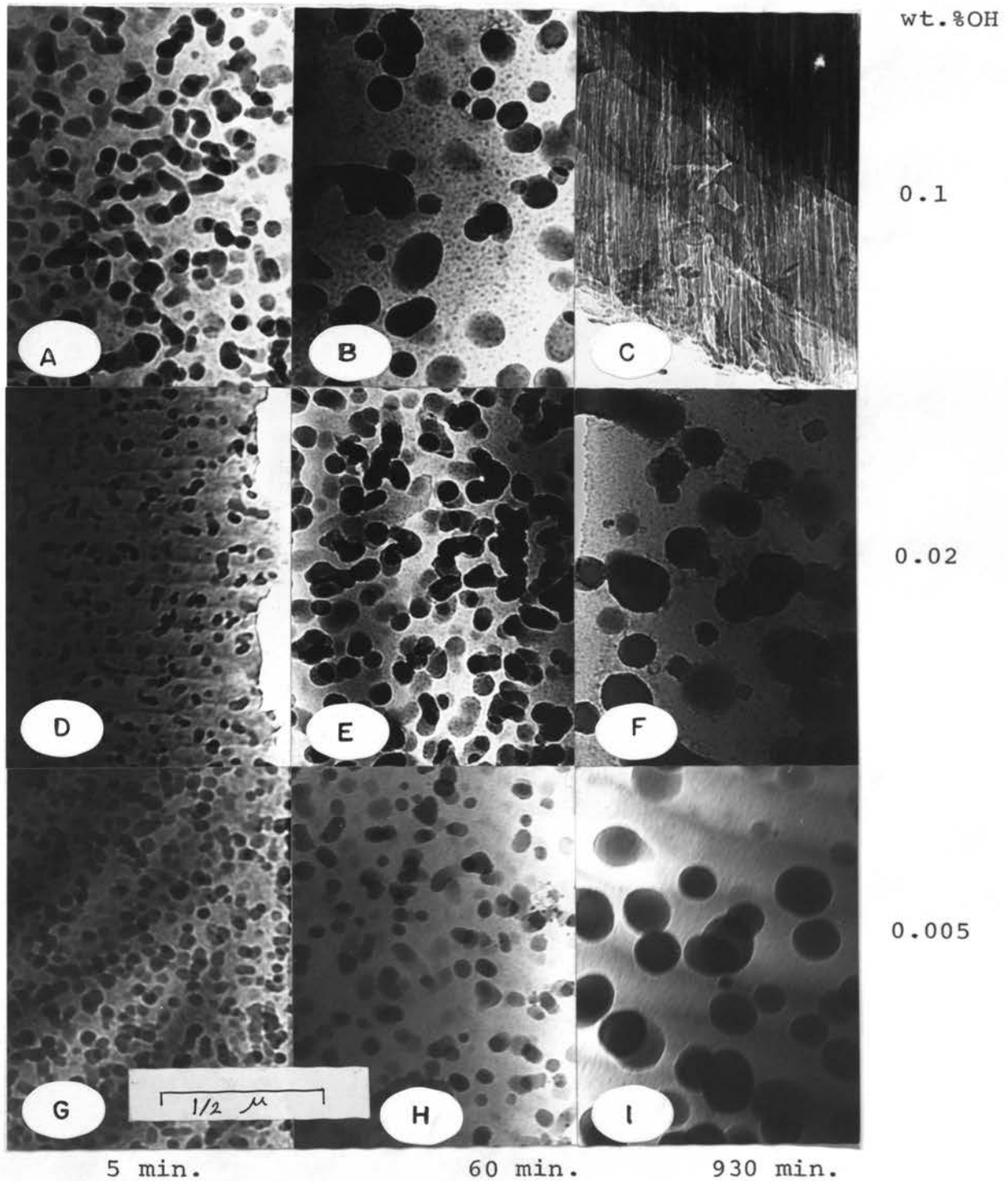
Figure 4.  Transmission electron micrographs for various heat treatments at 700°C, of glasses with different OH contents, 15.5 mol % $Na_2O$

(A,B,C) steam bubbling
(D,E,F) normal
(G,H,I) vacuum

wt. % OH

0.1

0.02

0.005

Quenched          12 min.
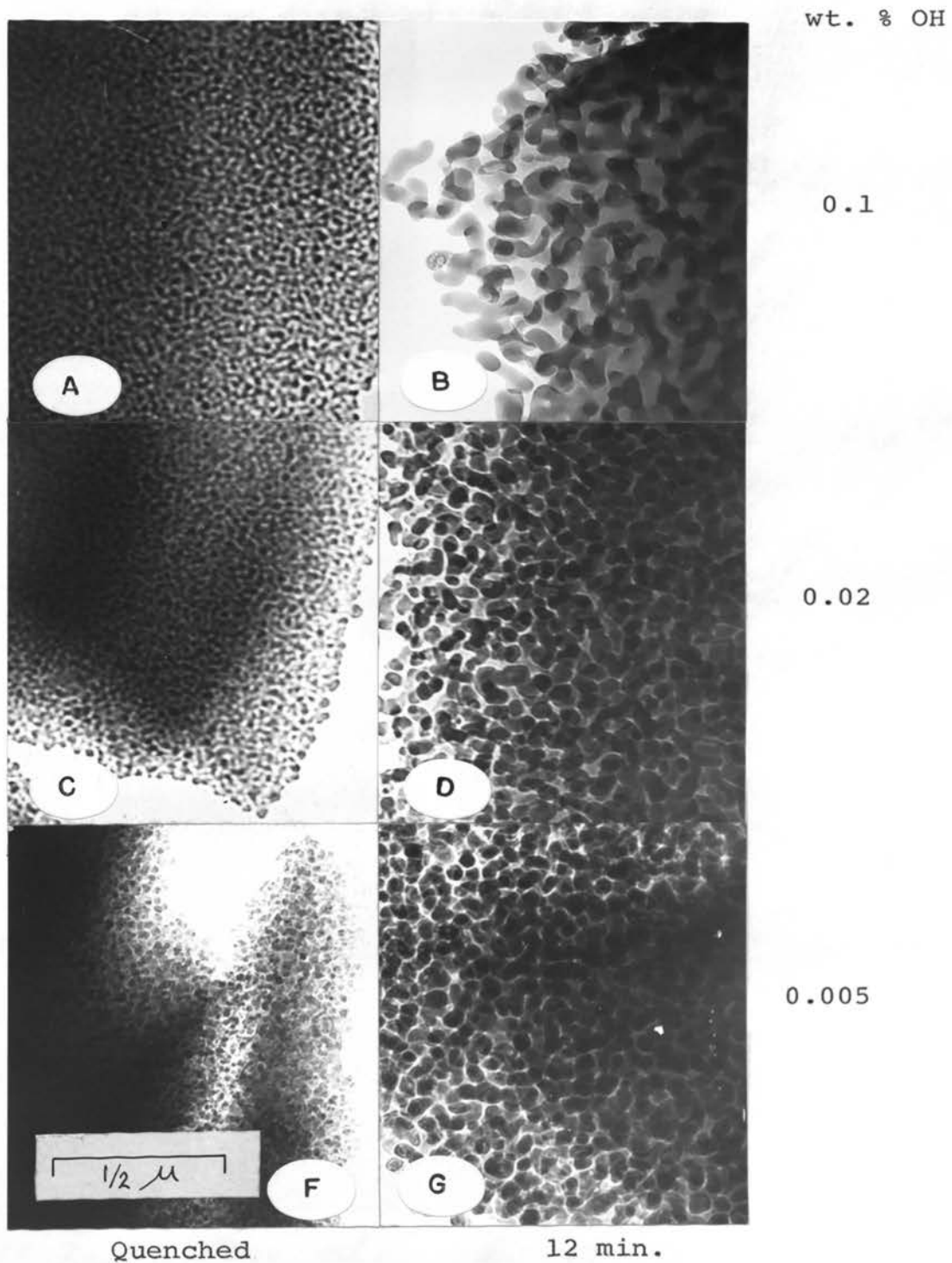
Figure 5.   Transmission electron micrographs for 12 min.
            heat treatment at 700°C of glasses with dif-
            ferent OH contents, 13 mol % Na₂O
            (A,B) steam bubbling  (C,D) normal
            (F,G) vacuum

REFERENCES FOR APPENDIX C

1.    W. Vogel, "Structure and Crystallization of Glass
      VEB DEUTSCHER VERLA GFUR GRUNDSTOF FINDUSTRIE,
      Leipzg (1965)

APPENDIX D

Determination of OH Concentration From Infrared Spectra

Infrared is considered to be one of the most useful
tools for estimating quantitatively the hydroxyl groups
in glass. It has long been known that the $H_2O$ molecule
exhibits very intensive absorption peaks at 2.9 and 6.2μ.
The 2.9μ peak is caused by O-H stretching vibrations,
whereas the 6.2μ peak is due to H-O-H bending vibrations.
The exact position of these peaks is related to the state
of aggregation. In silicate glasses, three characteristic
absorption bands, at about 2.9, 3.6 and 4.2μ, have been
assigned to be stretching vibration of OH groups with dif-
ferent degrees of hydrogen bonding[1].

To cut down the contribution of water absorbed on the
surfaces of the glass, the ground and polished samples
were heated for 24 hours under vacuum at 200°C. Samples
were then transferred to a desiccator, and measured on the
Perkin Elmer 377 I.R. spectrophotometer.

Two matching apertures were made for the sample and
the reference compartment; and the zero % and 100% trans-
mission were adjusted.

The absorption band position was determined from the
spectra corresponding to the highest water content; the
magnitude of absorption for 2.9 and 3.6μ bands was taken

from the chart and the background (the absorption on the shorter wave length side where there is no characteristic absorption) was subtracted from the measured absorption.

The calculation was carried out in a similar way as reported by Goetz and Vasahlova[2] on soda lime silica glass. They found that the Beers-Lambert law is valid for determining water content up to 0.11 mol % in glass, the extinction coefficient being 39.8 1/mole cm for the $3600 cm^{-1}$ band and 56.0 1/mole cm for the $2800 cm^{-1}$ band.

We assumed that the coefficient for the sodium silicate system will have the same order of magnitude but not necessarily the same value. The absorption coefficient is constant for glasses with the same composition, but will of course, vary with composition. However, the absorption coefficient for the $3600 cm^{-1}$ band was determined experimentally and was found to be 39.8 1/mol cm for soda-lime silica glass $(15:10:74)^{2)}$ and $49.1 \pm 2.55$ 1/mol cm for a completely different glass[3], of composition $SiO_2$ 50.86, $Al_2O_3$ 14.84, $B_2O_3$ 10.12, $CaO$ 17.95, $MgO$ 4.79, $Na_2O$ 0.98 and $BaO$ 0.17 in wt.%. In our experiment, where there is 10 mol % $Na_2O$ difference between the two extreme compositions, we could expect the change in absorption coefficient with composition would be less than 20%. We arbitrarily assumed similar absorption coefficients for sodium silicate glasses, 40 1/mol cm for $2.8\mu$ band and 55 1/mol cm for the $3.6\mu$ band, to make a semiquantitative comparison between glasses of the same composition.

Using Beers-Lambert's law the concentration in mol/1 will be

$$C = \frac{A}{KX}$$

C = concentration in mol/1

A = absorption

K = the extinction coefficient in 1/mol cm

X = the sample thickness in cm

The concentration in mol/1 can be converted to the concentration in wt.% using the equation:

$$\text{Conc.in wt.\%} = \frac{C \text{ X Molecular Wt. of OH(17) x 100}}{1000 \text{ x Glass Density}}$$

Example: Determination of OH content of the 13 mol % $Na_2O$ glass

| Glass | Absorption at 2.8μ | Absorption at 3.6μ |
|---|---|---|
| (1) melted under vacuum | 0.010 | .060 |
| (2) normal melting | 0.095 | .260 |
| (3) steam bubbling | 0.475 | .885 |

OH concentration mol/1
at 2.8μ                                    at 3.6μ

(1) $\dfrac{0.01}{40 \text{ x } 0.2023} = 0.0012$      $\dfrac{0.06}{55 \text{ x } 0.2023} = 0.0053$

(2) $\dfrac{0.095}{40 \text{ x } 0.2315} = 0.0102$      $\dfrac{0.26}{55 \text{ x } 0.2315} = 0.0204$

at 2.8μ                               at 3.6μ

$$(3) \quad \frac{0.475}{40 \times 0.1975} = 0.0601 \qquad\qquad \frac{0.885}{55 \times 0.1975} = 0.0814$$

| | OH Conc. (mol) | Density of Glass | OH Conc (wt.%) |
|---|---|---|---|
| (1) | 0.0065 | | 0.005 |
| (2) | 0.0306 | 2.32 | 0.023 |
| (3) | 0.1415 | | 0.109 |

The calculated OH content for glasses used in this study is shown in Table I. The infra-red spectra for these glasses is shown in Fig. (1) through (6).
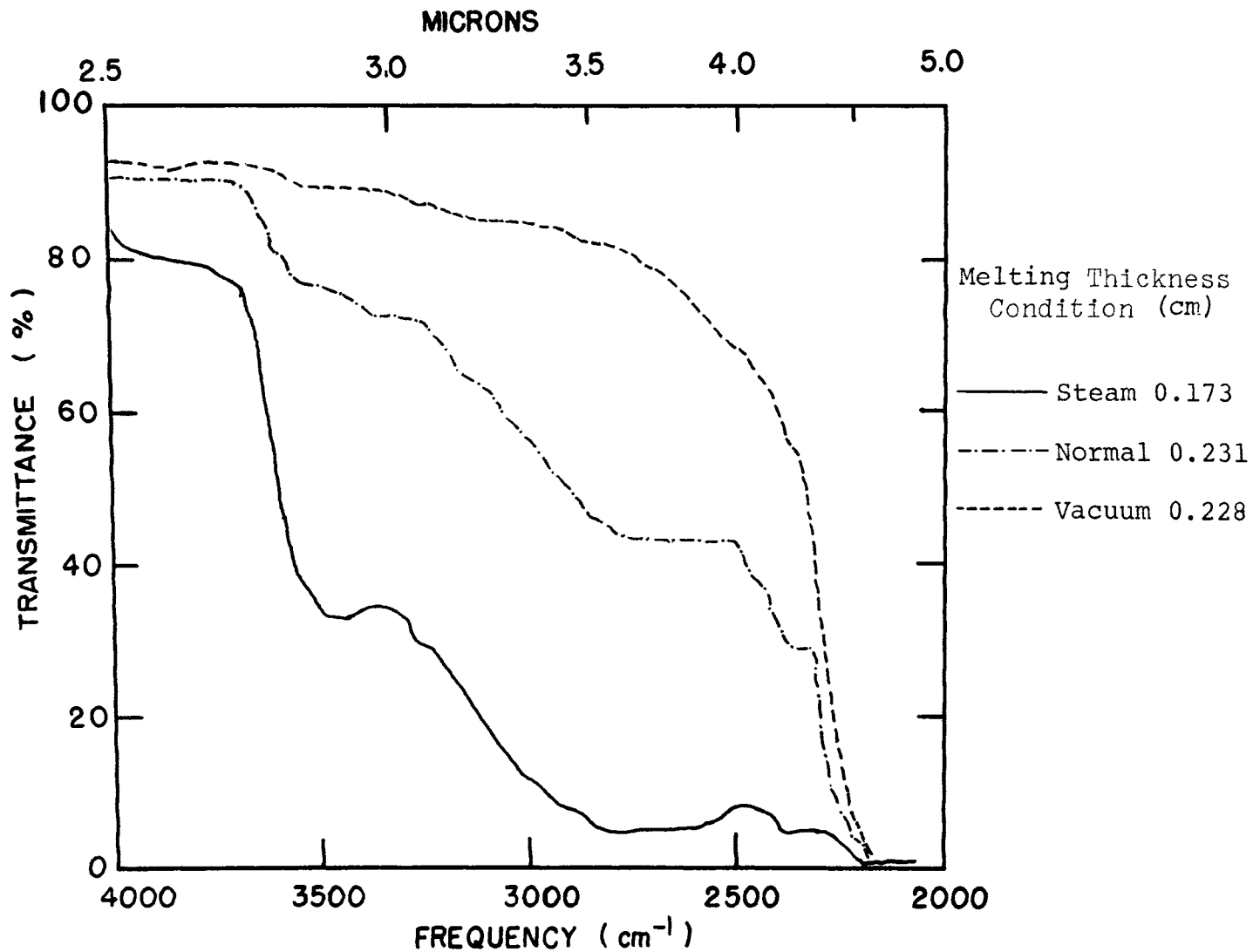
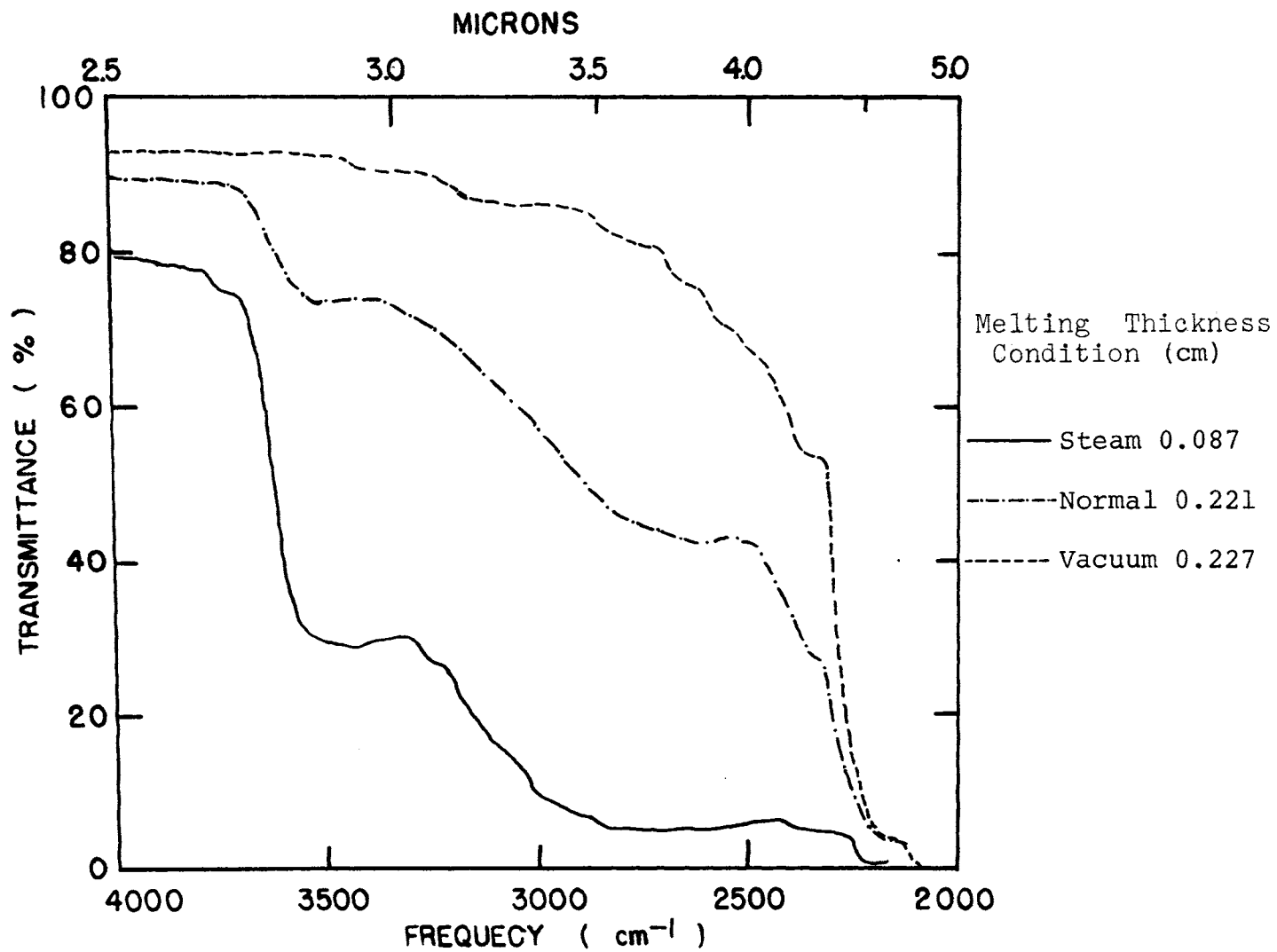Figure 1. Effect of melting condition on the infrared spectra of sodium silicate glasses [23 mol % $Na_2O$]

Figure 2. Effect of melting condition on the infrared spectra of sodium silicate glasses [20.5 mol % $Na_2O$]
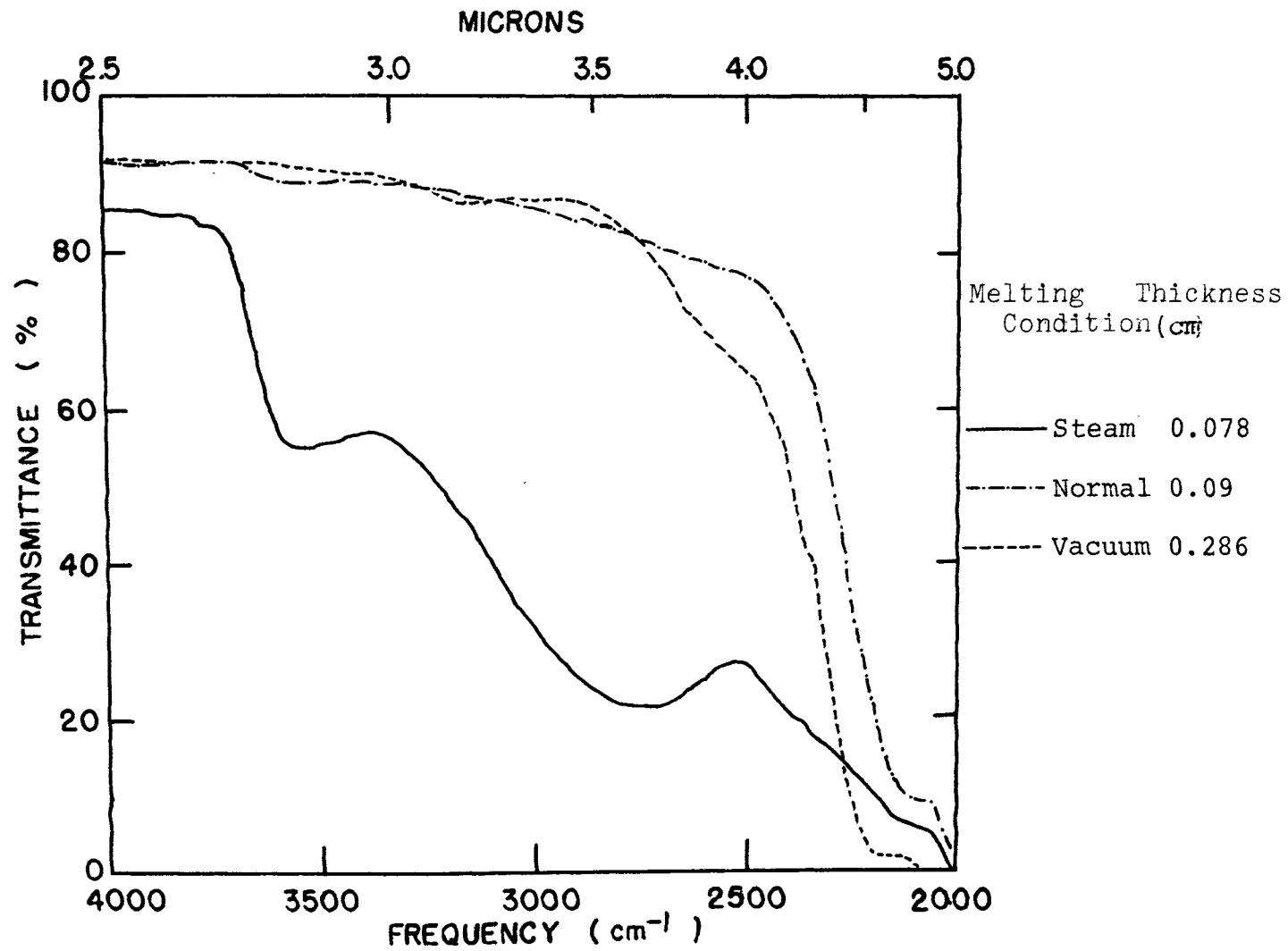
Figure 3. Effect of melting condition on the infrared spectra of sodium silicate glasses [18 mol % Na$_2$O]
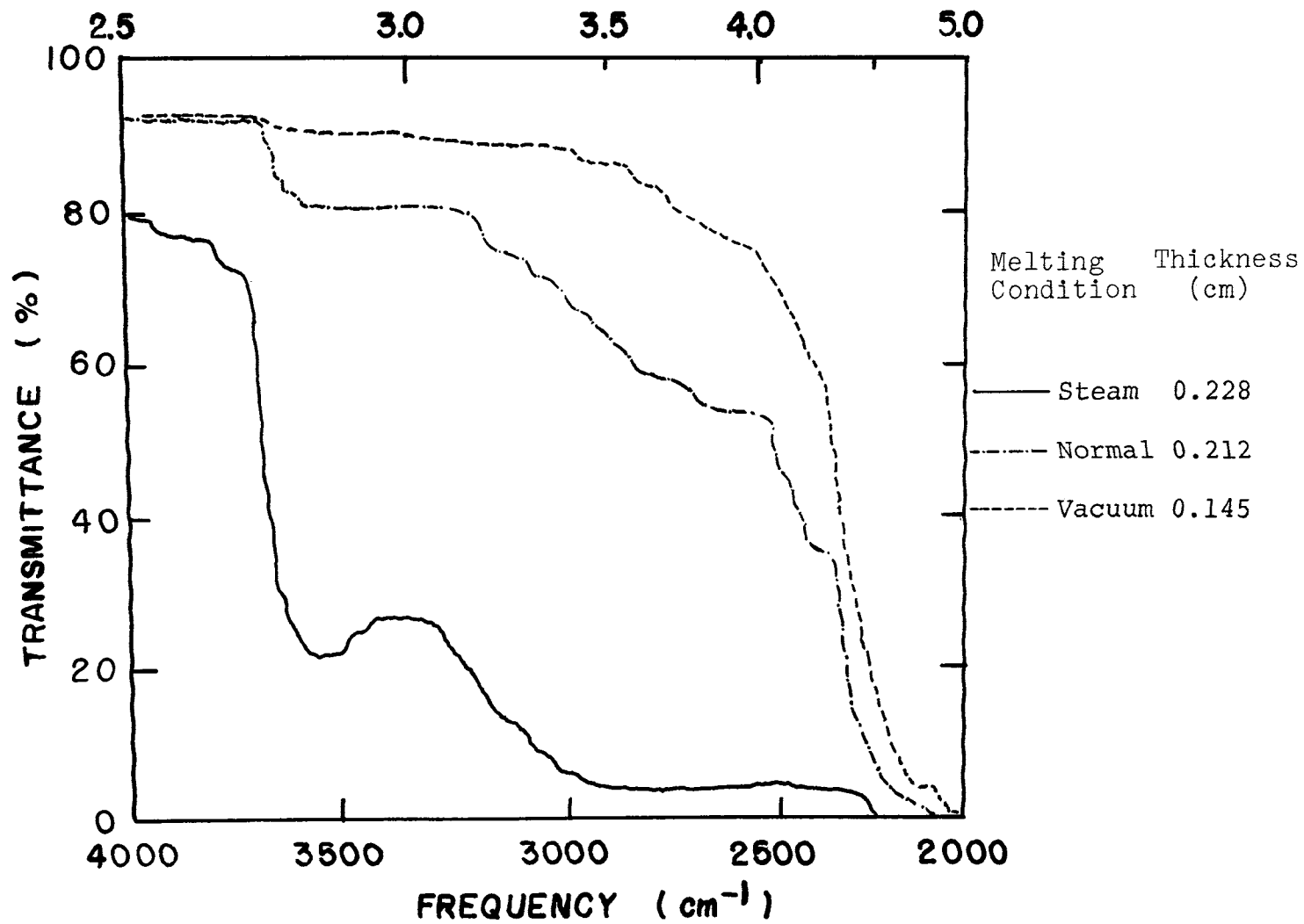
Figure 4. Effect of melting condition on the infrared spectra of sodium silicate glasses [15.5 mol % $Na_2O$]
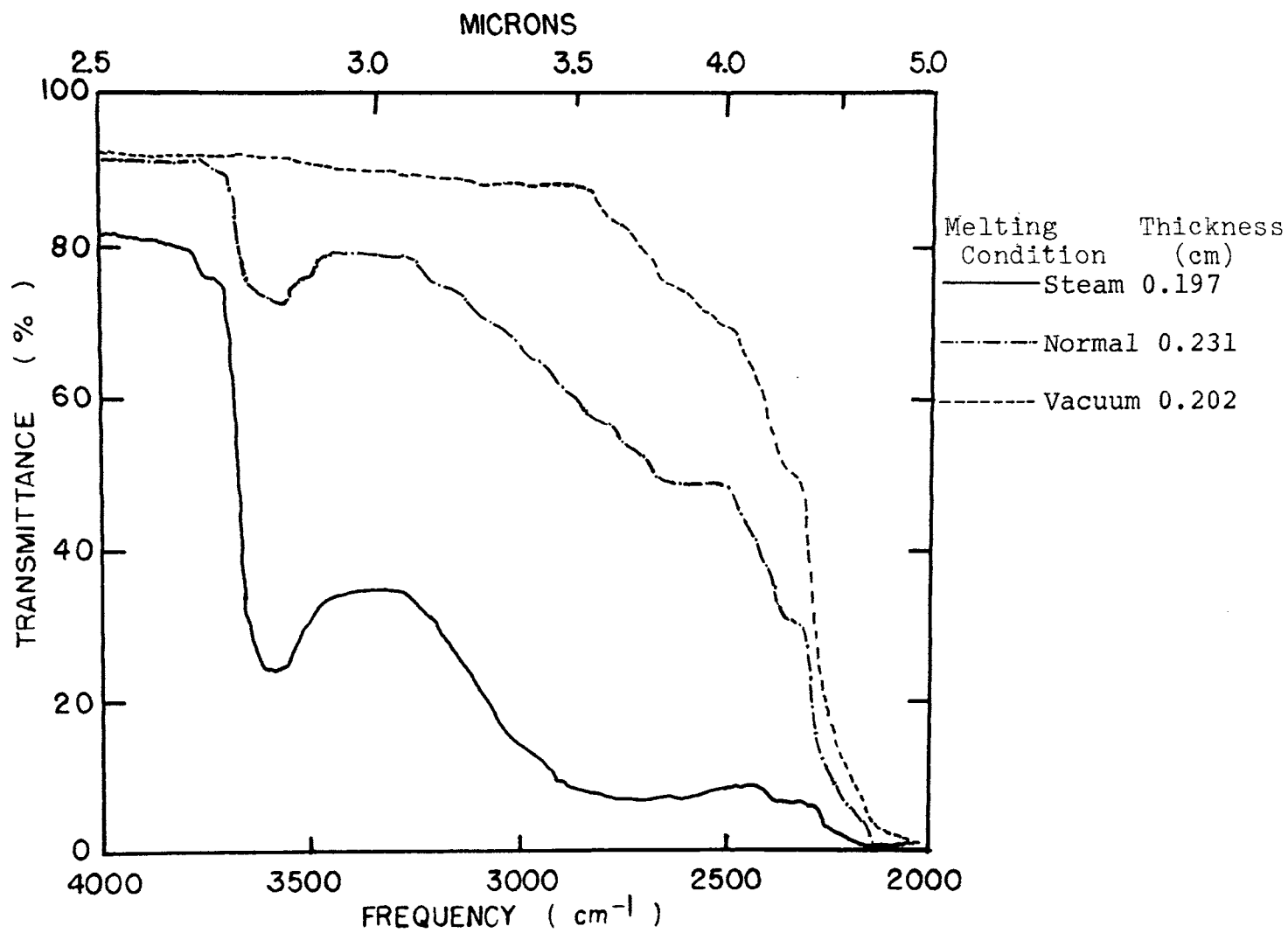
Figure 5.  Effect of melting condition on the infrared spectra of
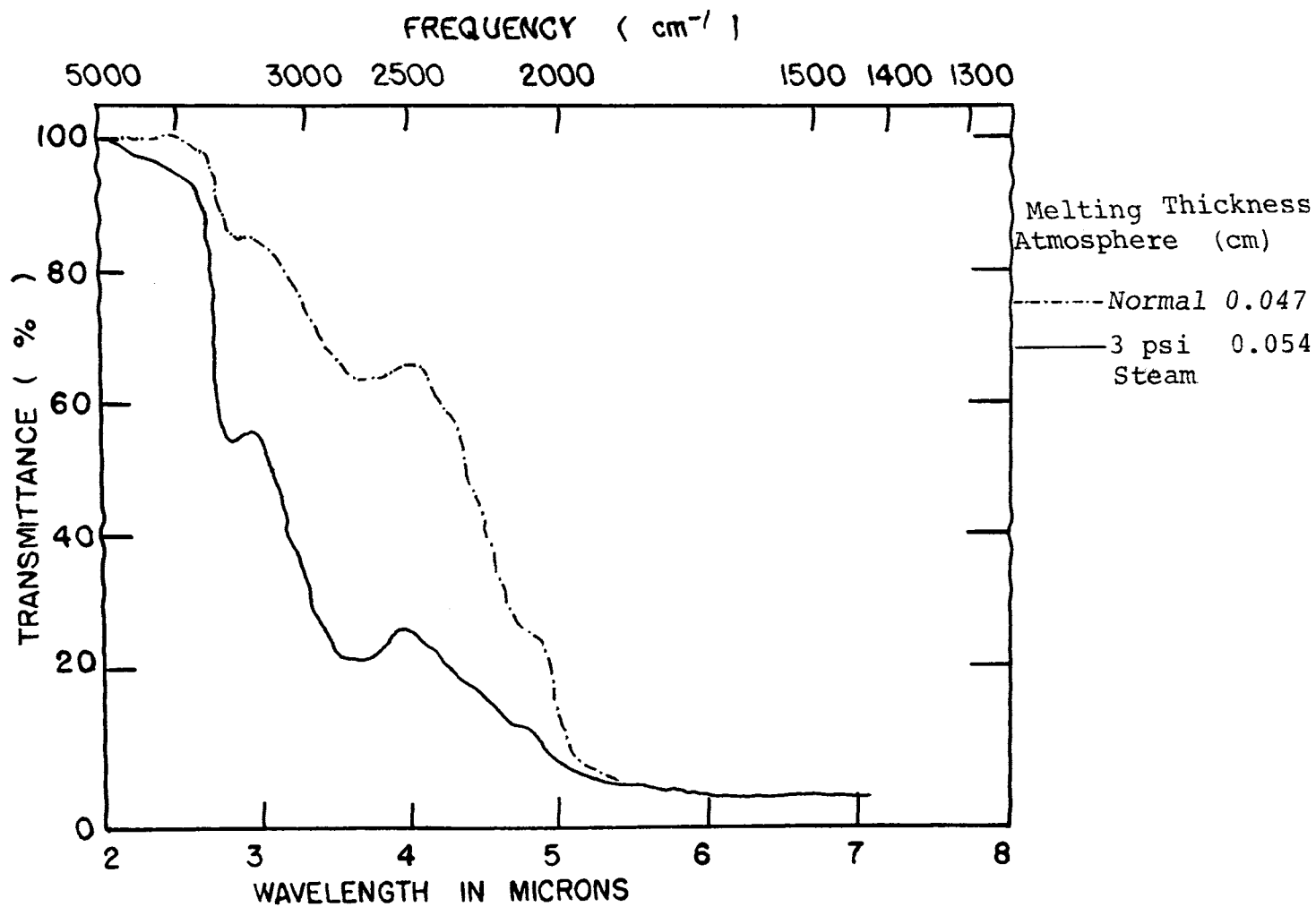sodium silicate glasses [13 mol % $Na_2O$]

Figure 6. Effect of melting condition on the infrared spectra of sodium silicate glasses [18 wt.% $Na_2O$]

TABLE I. The Calculated OH Content for Sodium
Silicated Glasses

| Composition | OH Concentration in wt% | | |
|---|---|---|---|
| (mol % $Na_2O$) | Steam bubbling | Normal | Vacuum Melting |
| 23 | 0.128 | .024 | .005 |
| 20.5 | 0.102 | .026 | .003 |
| 18 | 0.146 | .009 | .001 |
| 15.5 | 0.093 | .019 | .005 |
| 13 | 0.11 | .024 | .005 |

REFERENCES FOR APPENDIX D

1) SCHOLZE, H., Gases and water in glass. Glass Industry, 47, (1966) 624-625.

2) GOETZ, J., VOSAHLOVA, E., Quantitative determination of water content in glass with the aid of infrared OH bands, Glastech. Ber., 41, 2 (1968), 47-55.

3) NEMEC,L., GOETZ, J. Infrared absorption of OH$^-$ in E glass. J. Amer. Ceram. Soc. 53, 9 (1970), 526.

APPENDIX E

Internal Friction

Table I gives the values of the peak height and peak temperature for the alkali and high temperature peaks, in the 18 mol % $Na_2O$ sodium silicate glasses with different OH content, discussed earlier in Section 3.4.

| OH Content | ALKALI PEAK | | HIGH TEMPERATURE PEAK | |
|:---:|:---:|:---:|:---:|:---:|
| (wt.%) | Peak height x $10^3$ | Peak temperature $^\circ$C | Peak height x $10^3$ | Peak temperature $^\circ$C |
| 0.15 | 2.25 | 4. | 3.65 | 182 |
| 0.01 | 3.50 | -10 | 1.95 | 212 |
| 0.001 | 3.67 | -12 | 1.55 | 213 |

TABLE I. Effect of melting condition on the internal friction peak height and peak temperature in 18 mol % $Na_2O$ glass, Freq. = 0.4 Hz